

Research Article

A Novel Discrete-Time Leslie–Gower Model with the Impact of Allee Effect in Predator Population

S. Vinoth ¹, R. Sivasamy ², K. Sathiyathan ¹, B. Unyong ³, R. Vadivel ³
and Nallappan Gunasekaran ⁴

¹Department of Mathematics, SRMV College of Arts and Science, Coimbatore, TN, India

²Department of Science and Humanities, M.Kumarasamy College of Engineering, Karur, TN, India

³Department of Mathematics, Faculty of Science and Technology, Phuket Rajabhat University, Phuket 83000, Thailand

⁴Department of Advanced Science and Technology, Computational Intelligence Laboratory, Toyota Technological Institute, Nagoya 468-8511, Japan

Correspondence should be addressed to B. Unyong; bundit.u@pkru.ac.th

Received 11 October 2021; Revised 23 December 2021; Accepted 1 February 2022; Published 28 March 2022

Academic Editor: C. Rajivganthi

Copyright © 2022 S. Vinoth et al. This is an open access article distributed under the Creative Commons Attribution License, which permits unrestricted use, distribution, and reproduction in any medium, provided the original work is properly cited.

The discrete-time system has more complex and chaotic dynamical behaviors as compared to the continuous-time system. This paper extends a discrete Leslie–Gower predator-prey system with the Allee effect in the predator's population, whose dynamics are analyzed and explored. We have determined the equilibrium points and studied their local stability properties. We find that the system undergoes flip bifurcation and Neimark–Sacker bifurcation around the interior equilibrium point by choosing the Allee parameter as a bifurcation parameter. We discuss the stability and direction of both bifurcations with the help of the normal form theory and center manifold theorem. The flip bifurcation and Neimark–Sacker bifurcation are the most common routes to the chaotic orbit in the discrete system. Moreover, we utilize state feedback, pole placement, and hybrid control methods to control the chaos in the system. The work is complete with the numerical simulations to confirm the analytical findings.

1. Introduction

The study of interactions between prey and predator has particular interest for many mathematicians and ecologists. Many researchers investigated the dynamic behavior of the predator-prey system and contributed to the development of continuous-time systems. Another possible way to understand the complex problem of two interacting species is by discrete systems [1]. Moreover, it has been observed that the discrete-time systems are more appropriate than the continuous-time systems for the populations with nonoverlapping generations [2]. The discrete-time models are more appropriate and provide efficient results than continuous models for small-size populations [3]. For example, the discrete model is better for studying insect populations since there is only one generation per year and an annual plant population because there are no overlapping generations annually. Jing and Yang [4], Liu and Xiao [5], and Elabbasy

et al. [6] showed that the discrete-time system showed richer and more complex dynamics compared to the continuous-time systems. Many researchers formulated and studied the discrete-time predator-prey system by implementing the forward Euler scheme [4, 5, 7], nonstandard finite difference scheme [8, 9], and piecewise constant arguments [10–12]. For instance, the authors in [13] obtained a discrete-time predator-prey system with a crowding effect and predator partially dependent on prey by applying the forward Euler's scheme from the continuous-time system. They also showed the existence of a cascade of period-doubling bifurcation and Hopf bifurcation in the considered system. On the other hand, Abbasi et al. [12] used the method of piecewise constant arguments and obtained the discrete system. Also, the authors investigated stability, bifurcations, and chaos control analysis. In [14], the authors investigated the discrete-time predator-prey system with hunting cooperation through numerical simulation and observed that the system

undergoes both types of bifurcations. In [15], the authors discussed the chaotic dynamics of a discrete prey-predator system with Holling-II type functional response. The other fruitful results on discrete-time models can be found in [16, 17].

The Allee effect is a biological phenomenon named after Allee [18], who was the first to write thoroughly about it. It denotes the presence of a positive relationship between population size and per capita growth rate. This effect usually saturates or vanishes as the population expands. There has been a great deal of literature on deriving continuous-time prey-predator models with the Allee effect [19–22]. The impact of the Allee effect in the discrete-time prey-predator models has also been studied in the literature [23–26]. For example, Celik and Duman [23] studied the impact of the Allee effect in the discrete-time predator-prey model with linear interaction. They showed that the Allee effect on prey population changes the unstable equilibrium into a stable state. In [25], the authors studied the discrete-time predator-prey model with strong and weak Allee effects. Also, they showed that the chaotic orbits appear for larger step size values through period-doubled orbits and invariant circle orbits. AlSharawi et al. [26] considered the Allee effect in the discrete-time prey-predator model with a nonmonotonic functional response. They performed the stability analysis and provided conditions for the occurrence of flip and Neimark–Sacker bifurcations by taking the Allee parameter as a bifurcation parameter. Also, they showed that the system has two types of bistability behaviors.

Several research works have been done for bifurcation and chaos control in nonlinear systems. It refers to the role of constructing a controller to alter the chaotic and bifurcating properties of a given nonlinear system to achieve some desired dynamical behaviors [27–30]. One can shift the chaotic attractor to any one of a large number of possible attracting periodic motions, as in [31]. Recently, the studies on bifurcation and chaos control in the discrete-time predator-prey models attained much more interest among researchers. For example, Din [32] showed that the model undergoes flip bifurcation (FB) and Neimark–Sacker bifurcation (NSB) for larger values of the growth rate of the prey population. Furthermore, the author implemented three different types of control strategies to control the chaos. Moreover, for some interesting results related to bifurcation and chaos control in the predator-prey models, we refer the readers to [33–35].

Motivated by the above-mentioned works, we consider the modified Leslie–Gower prey-predator system introduced by Alaoui and Okiye in [36] by assuming that the growth rate of the predator is affected by the presence of the Allee effect. Also, the prey and predator populations have nonoverlapping generations. The discrete-time model is obtained by the method of piecewise constant arguments for the differential equation [10–12] from its corresponding continuous-time system. We attempt to study the discrete-time system and observe some rich dynamics that the continuous-time system does not have. Feng and Kang [20] investigated the [36] continuous-time model with an Allee effect in both prey and predator. To the best of our knowledge, there has been less

research done in discrete predator-prey systems with the Allee effect in the predator population. The main purpose of this paper is to show the rich dynamics of the discrete system in terms of bifurcations (FB and NSB) and chaos by taking the Allee parameter as a bifurcation parameter. Flip and Neimark–Sacker bifurcations are the common routes to chaos in discrete systems. Additionally, if the discrete system is chaotic under certain parametric conditions, we can use various control methods to stabilize the chaotic orbits near the unstable equilibrium point. It is worth mentioning here that the study on stability, bifurcation, and chaos control analysis for the prey-predator model with Allee effect in predator population is different from the whole of the existing works.

This paper is organized as follows: in Section 2, we describe the formation of a discrete-time system for populations with nonoverlapping generations from the continuous counterpart. In Section 3, we study the existence and local stability of the equilibrium points for the discrete-time system. In Section 4, we illustrate the existence of flip and Neimark–Sacker bifurcation by taking the Allee parameter as a bifurcation parameter. Section 5 is related to the implementation of state feedback, pole-placement, and hybrid control methods to delay the chaos in the system. Lastly, to ensure our analytical results, the various numerical simulations are performed in Section 6.

2. Model Formulation

Firstly, we describe the continuous-time predator-prey system of modified Leslie–Gower with Holling type II functional response. It was introduced by Alaoui and Okiye in [36], which is of the following form:

$$\begin{cases} \frac{dx(t)}{dt} = x(t) \left(r_1 - ax(t) - \frac{gy(t)}{x(t)+b} \right), \\ \frac{dy(t)}{dt} = y(t) \left(r_2 - \frac{hy(t)}{x(t)+c} \right). \end{cases} \quad (1)$$

$x(0) \geq 0$ and $y(0) \geq 0$, where $x(t)$ and $y(t)$ represent the population sizes of prey and predator at time t . r_1 , a , g , b , r_2 , h , and c are all positive constants. r_1 and r_2 are the growth rates of x and y . a measures the strength of competition among the individuals of species x . g is the maximum value a per capita reduction rate of x can attain. b (respectively, c) measures the extent to which the environment provides protection to prey x (respectively, to predator y), and h has a similar meaning to g . The assumption that the amount to which the environment provides protection to both the predator and the prey is the same (i.e., $b = c$) has been considered in [37, 38]. Singh et al. [39] extended system (1) with the death rate of predators, obtained a discrete system by Euler's method, and also considered step size as a bifurcation parameter. This fact violates the numerical method of discretization. To overcome this, Din in [32] applied the method of piecewise constant arguments to obtain the discrete system. Recently, the discrete version of system (1)

was derived using Euler's method with step size 1 by the authors in [40] and showed bifurcation behavior with other model parameters.

Now, we consider that system (1) is subject to the Allee effect in predator population, and it is given by

$$\begin{cases} \frac{dx(t)}{dt} = x(t)(r_1 - ax(t)) - \frac{gx(t)y(t)}{x(t)+b}, \\ \frac{dy(t)}{dt} = y(t)\left(\frac{r_2y(t)}{y(t)+m} - \frac{hy(t)}{x(t)+c}\right), \end{cases} \quad (2)$$

where $y(t)/m + y(t)$ is the Allee effect term and $m > 0$ represents the severity of Allee effect in the predator population. The authors in [41] studied system (2) with ratio-dependent functional response and the fear in prey population.

Next, based on the appropriate modifications of overlapping generations, one can get the difference equation for modeling population with nonoverlapping generations. We aim to study the populations that have nonoverlapping generations for system (2). Moreover, it is necessary to obtain the discrete-time system from its continuous counterpart. In this way, the method of piecewise constant argument has been useful. The corresponding discrete-time system (2) is obtained by the method of piecewise constant arguments for the differential equations [10–12, 14], assuming that the populations have no overlap between successive generations and the population growth occurs in discrete steps $t \in [n, n+1)$, $n = 0, 1, 2, \dots$. Let us consider that the variables and constants in (2) change in the regular time intervals and obtain the following modified system:

$$\begin{cases} \frac{1}{x(t)} \frac{dx(t)}{dt} = r_1 - ax(t) - \frac{gy(t)}{x(t)+b}, \\ \frac{1}{y(t)} \frac{dy(t)}{dt} = \frac{r_2y(t)}{y(t)+m} - \frac{hy(t)}{x(t)+c}, \end{cases} \quad t \neq 0, 1, 2, \dots, \quad (3)$$

where $[t]$ is the integer part of t , $t \in (0, +\infty)$. On any interval of the form $[n, n+1)$, $n = 0, 1, 2, \dots$, we can integrate (3) and obtain the following:

$$\begin{cases} \ln \frac{x(t)}{x(n)} = \left[r_1 - ax(n) - \frac{gy(n)}{x(n)+b} \right] (t-n), \\ \ln \frac{y(t)}{y(n)} = \left[\frac{r_2y(n)}{y(n)+m} - \frac{hy(n)}{x(n)+c} \right] (t-n), \end{cases} \quad n = 0, 1, 2, \dots \quad (4)$$

By simplification and letting $t \rightarrow n+1$, the corresponding discrete-time system for (2) is obtained by the method of piecewise constant arguments for differential equations can be written as follows:

$$\begin{cases} x(n+1) = x(n) \exp \left[r_1 - ax(n) - \frac{gy(n)}{x(n)+b} \right], \\ y(n+1) = y(n) \exp \left[\frac{r_2y(n)}{y(n)+m} - \frac{hy(n)}{x(n)+c} \right], \end{cases} \quad (5)$$

where $x(n+1)$ and $y(n+1)$ denote the populations in generation $n+1$, and they are related to the sizes $x(n)$ and $y(n)$ of the populations in the preceding generation n . Note that in the absence of a predator, system (5) reduces to the one-dimensional system, similar to the Ricker model [16]. Thus, this current article aims to analyze the local stability, bifurcation, and chaos control analyses for the discrete system (5) that models the interaction between populations that have nonoverlapping generations.

3. The Existence and Local Stability of the Equilibria

3.1. The Equilibria. To find the equilibrium points of system (5), we use direct substitution method to solve the following equations:

$$r_1 - ax - \frac{gy}{x+b} = 0, \quad \frac{r_2}{y+m} - \frac{h}{x+c} = 0. \quad (6)$$

Form the above equations, we have the following points of equilibria:

The origin $E_0 = (0, 0)$.

The predator-free equilibrium $E_1 = (\bar{x}, 0) = (r_1/a, 0)$.

The prey-free equilibrium $E_2 = (0, \bar{y}) = (0, r_2c/h - m)$ exists if $r_2c/h > m$.

The interior equilibrium point is $E^*(x^*, y^*)$, where $y^* = r_2x^*/h + r_2c - mh/h$ and x^* is the positive root of the following equation:

$$ahx^{*2} + (abh + gr_2 - r_1h)x^* + g(r_2c - mh) - r_1hb = 0, \quad (7)$$

If $r_2c - mh/h < r_1b/g$ holds, then (6) has at least one positive real root x^* .

To guarantee the existence of interior equilibrium point $E^*(x^*, y^*)$, we need the following lemma.

Lemma 1. *Let us assume that $r_2c - mh/h < r_1b/g$ and $r_2(x^* + c) > mh$ always hold. Then, $E^*(x^*, y^*)$ is the unique positive interior equilibrium point of system (5).*

3.2. Local Stability Analysis. To analyze the local stability properties of the equilibria, we need the Jacobian matrix at an arbitrary equilibrium $E(x, y)$, which is given as follows:

$$J = \begin{pmatrix} \left(1 - ax + \frac{gxy}{(x+b)^2}\right)A_1 & \frac{-gx}{x+b}A_1 \\ \frac{hy^2}{(c+x)^2}A_2 & \left(1 - \frac{hy}{c+x} + \frac{r_2my}{(y+m)^2}\right)A_2 \end{pmatrix}, \quad (8)$$

where $A_1 = \exp[r_1 - ax - gy/x + b]$ and $A_2 = \exp[r_2y/y + m - hy/x + c]$.

Then, we have the subsequent lemmas for the local stability analysis of the equilibria.

Lemma 2. For system (5), we have,

- (1) E_0, E_1 are nonhyperbolic points.
- (2)

- (a) $E_2(0, \bar{y})$ is a sink if $|\exp(r_1 - g\bar{y}/b)| < 1$ and $|(1 - h\bar{y}/c + r_2m\bar{y}/(\bar{y} + m)^2)A_3| < 1$.
- (b) $E_2(0, \bar{y})$ is a source if $|\exp(r_1 - g\bar{y}/b)| > 1$ and $|(1 - h\bar{y}/c + r_2m\bar{y}/(\bar{y} + m)^2)A_3| < 1$.
- (c) $E_2(0, \bar{y})$ is a saddle if $|\exp(r_1 - g\bar{y}/b)| < 1$, $|(1 - h\bar{y}/c + r_2m\bar{y}/(\bar{y} + m)^2)A_3| < 1$, $|\exp(r_1 - g\bar{y}/b)| < 1$, and $|(1 - h\bar{y}/c + r_2m\bar{y}/(\bar{y} + m)^2)A_3| > 1$.
- (d) $E_2(0, \bar{y})$ is a nonhyperbolic if $|\exp(r_1 - g\bar{y}/b)| = 1$ or $|(1 - h\bar{y}/c + r_2m\bar{y}/(\bar{y} + m)^2)A_3| = 1$.

Proof. The Jacobian matrix at $E_0(0, 0)$ is as follows:

$$J_{E_0} = \begin{pmatrix} \exp(r_1) & 0 \\ 0 & 1 \end{pmatrix}, \quad (9)$$

with the eigenvalues $\lambda_{1,2} = \exp(r_1), 1$.

The Jacobian matrix at $E_1(\bar{x}, 0)$ is as follows:

$$J_{E_1} = \begin{pmatrix} 1 - r_1 & \frac{gr_1}{ab + r_1} \\ 0 & 1 \end{pmatrix}, \quad (10)$$

with the eigenvalues $\lambda_{1,2} = \exp(1 - r_1), 1$.

The Jacobian matrix at $E_2(0, \bar{y})$ is as follows:

$$J_{E_2} = \begin{pmatrix} \exp\left(r_1 - \frac{g\bar{y}}{b}\right) & 0 \\ \frac{h\bar{y}^2}{c^2}A_3 & \left(1 - \frac{h\bar{y}}{c} + \frac{r_2m\bar{y}}{(\bar{y} + m)^2}\right)A_3 \end{pmatrix}, \quad (11)$$

with $A_3 = \exp[r_2\bar{y}/\bar{y} + m - h\bar{y}/c]$, and the eigenvalues are $\lambda_1 = \exp(r_1 - g\bar{y}/b)$ and $\lambda_2 = (1 - h\bar{y}/c + r_2m\bar{y}/(\bar{y} + m)^2)A_3$. \square

Lemma 3. The interior equilibrium point

- (a) $E^*(x^*, y^*)$ is a sink if $B_2 < 1$ and $|B_1| < B_2 + 1$.
- (b) $E^*(x^*, y^*)$ is a source if $B_2 > 1$ and $|B_1| < B_2 + 1$ or $|B_1| > B_2 + 1$.
- (c) $E^*(x^*, y^*)$ is a saddle if $0 < |B_1| + B_2 + 1 < 2|B_1|$.

- (d) $E^*(x^*, y^*)$ is nonhyperbolic if $|B_1| = |B_2 + 1|$, or $B_2 = 1$, and $|B_1| \leq 2$.

Proof. The Jacobian matrix at $E^*(x^*, y^*)$ is as follows:

$$J_{E^*} = \begin{pmatrix} 1 - ax^* + \frac{gx^*y^*}{(x^* + b)^2} & \frac{gx^*}{x^* + b} \\ \frac{hy^{*2}}{(x^* + c)^2} & 1 - \frac{r_2y^{*2}}{(y^* + m)^2} \end{pmatrix}. \quad (12)$$

Then, the characteristic polynomial of J_{E^*} is as follows:

$$F(\lambda) := \lambda^2 - B_1\lambda + B_2 = 0, \quad (13)$$

where

$$B_1 = 2 - ax^* + \frac{gx^*y^*}{(x^* + b)^2} - \frac{r_2y^{*2}}{(y^* + m)^2},$$

$$B_2 = \left(1 - ax^* + \frac{gx^*y^*}{(x^* + b)^2}\right) \left(1 - \frac{r_2y^{*2}}{(y^* + m)^2}\right) + \frac{ghx^*y^{*2}}{(x^* + b)(x^* + c)^2}. \quad (14)$$

\square

3.3. Bistability. Since model (5) is with the Allee effect in predator population, it is possible for the occurrence of bistability criteria, which is for two positive equilibrium points to exist and for both to be stable. From Lemma 2, E_0 and E_1 are nonhyperbolic points. The only possibility is between E_2 and E^* . Also, from Lemma 1, E_2 exists if $r_2c/h > m$, and E^* exists if $r_2c - mh/h < r_1b/g$ and $r_2(x^* + c) > mh$ holds. If $r_2c - mh/h < r_1b/g$, then E_2 is unstable form Lemma 2 (a), since one of the eigenvalues of J_{E_2} is $|\exp(r_1 - \bar{y}/b)| > 1$. Then, we can say that if E^* exists, then E_2 is unstable. Hence, there is less possibility for the occurrence of bistability for model (5).

4. Bifurcation Analysis

We have studied the stability properties of $E^*(x^*, y^*)$ previously. In the subsequent section, we choose the Allee parameter m as a bifurcation parameter to analyze the bifurcation behaviour of system (5). We derive the conditions to obtain flip bifurcation (FB) and Neimark–Sacker bifurcation (NSB) at $E^*(x^*, y^*)$. Moreover, we utilize the center manifold theorem and the normal form theory [42, 43] to discuss the direction and stability property of the flip bifurcation and Neimark–Sacker bifurcation at $E^*(x^*, y^*)$.

4.1. Flip Bifurcation. System (5) undergoes flip bifurcation if one of the eigenvalues of J_{E^*} must be -1 and the other should not be 1 or -1 . Using this, we assume one of the

eigenvalues of J_{E^*} as -1 . Then, from (12)₂ we have the following:

$$F(-1) := 4 - 2ax^* - \frac{2r_2y^{*2}}{(y^* + m)^2} + \frac{2gx^*y^*}{(x^* + b)^2} + \frac{ar_2x^*y^{*2}}{(y^* + m)^2} + \frac{ghx^*y^{*2}}{(x^* + b)(x^* + c)^2} - \frac{gr_2x^*y^{*3}}{(x^* + b)^2(y^* + m)^2} = 0. \quad (15)$$

Note that the left-hand side of expression (13) is in terms of parameter m in denominator with power. Hence, it is difficult to find the explicit value of m for which system (5) undergoes flip bifurcation. Hence, we denote $m = m_h$ as the critical parameter value that satisfies (13). Also, $E^*(x^*, y^*)$ is derived at the critical value $m = m_f$.

Next, if $a_2 > 0$, $a_3 < 0$, and $h(y^* + m)/r_2 > c$ holds, we define that the neighborhood Θ_f for system (5) undergoes flip bifurcation near the equilibrium point E^* at some critical value $m = m_f$ as follows:

$$\Theta_f = \{(r_1, r_2, a, b, c, g, h, m) : m = m_f, r_1, r_2, a, b, c, g, h > 0\}. \quad (16)$$

Hence, we assume that system (5) undergoes flip bifurcation when $m = m_f$ changes in the neighborhood Θ_f .

Now, we investigate the direction and stability of the possible occurrence of flip bifurcation for system (5) at $E^*(x^*, y^*)$ with the steps followed in [32, 42]. Since, $(r_1, r_2, a, b, c, g, h, m) \in \Theta_f$ on giving a perturbation $|m_1| \ll 1$ of critical value $m = m_f$ for which system (5) undergoes flip bifurcation, then the perturbation system is given by the following:

$$\begin{cases} x_{n+1} = x_n \exp \left[r_1 - ax_n - \frac{gy_n}{x_n + b} \right], \\ y_{n+1} = y_n \exp \left[\frac{r_2y_n}{y_n + m_1 + m_f} - \frac{hy_n}{x_n + c} \right]. \end{cases} \quad (17)$$

Next, we transform the equilibrium point $E^*(x^*, y^*)$ into the origin by letting $p_n = x_n - x^*$ and $q_n = y_n - y^*$. Form (17), we obtain the following:

$$\begin{cases} p_{n+1} = (p_n + x^*) \exp \left[r_1 - a(p_n + x^*) - \frac{g(q_n + y^*)}{(p_n + x^*) + b} \right] - x^*, \\ q_{n+1} = (q_n + y^*) \exp \left[\frac{r_2(q_n + y^*)}{(q_n + y^*) + (m_1 + m_f)} - \frac{h(q_n + y^*)}{(p_n + x^*) + c} \right] - y^*. \end{cases} \quad (18)$$

By Taylor's series expansion, (16) becomes,

$$\begin{cases} p_{n+1} = \alpha_1 p_n + \alpha_2 q_n + \alpha_3 m_1 + \alpha_4 p_n^2 + \alpha_5 q_n^2 + \alpha_6 m_1^2 + \alpha_7 p_n q_n \\ \quad + \alpha_8 p_n m_1 + \alpha_9 q_n m_1 + o\left(\left(|p_n| + |q_n| + |m_1|\right)^2\right), \\ q_{n+1} = \beta_1 p_n + \beta_2 q_n + \beta_3 m_1 + \beta_4 p_n^2 + \beta_5 q_n^2 + \beta_6 m_1^2 + \beta_7 p_n q_n \\ \quad + \beta_8 p_n m_1 + \beta_9 q_n m_1 + o\left(\left(|p_n| + |q_n| + |m_1|\right)^2\right), \end{cases} \quad (19)$$

where

$$\begin{aligned}
\alpha_1 &= 1 + x^* M_1, \alpha_2 = \frac{-gx^*}{x^* + b}, \alpha_3 = 0, \alpha_4 = \frac{-gx^* y^*}{(x^* + b)} + M_1 \frac{x^*}{2} M_1^2, \\
\alpha_5 &= \frac{g^2 x^*}{2(x^* + b)^2}, \alpha_6 = 0, \alpha_7 = \frac{-gb}{(x^* + b)^2} - \frac{gM_1 x^*}{x^* + b}, \alpha_8 = 0, \alpha_9 = 0, \\
\beta_1 &= \frac{hy^{*2}}{(x^* + c)^2}, \beta_2 = 1 + y^* M_2, \beta_3 = -\frac{r_2 y^{*2}}{(y^* + m_f)^2}, \\
\beta_4 &= \frac{-hy^{*2}}{(x^* + c)^3} + \frac{h^2 y^{*3}}{2(x^* + c)^4}, \beta_5 = \frac{-r_2 m_f y^*}{(y^* + m_f)^3} + M_2 + \frac{y^* M_2^2}{2}, \\
\beta_6 &= \frac{r_2^2 y^{*3}}{2(y^* + m_f)^4} + \frac{r_2 y^{*2}}{(y^* + m_f)^3}, \beta_7 = \frac{2hy^*}{(x^* + c)^2} + \frac{hy^{*2} M_2}{(x^* + c)^2}, \\
\beta_8 &= \frac{-hr_2 y^{*3}}{(x^* + c)^2 (y^* + b)^2}, \beta_9 = \frac{-2m_f r_2 y^*}{(y^* + m_f)^3} - \frac{r_2 M_2 y^{*2}}{(y^* + m_f)^2}, \\
M_1 &= -\alpha + \frac{gy^*}{(x^* + b)^2}, M_2 = \frac{-r_2 y^*}{(y^* + m_f)^2}.
\end{aligned} \tag{20}$$

Consider

$$J_{E^*} = \begin{pmatrix} 1 - ax^* + \frac{gx^* y^*}{(x^* + b)^2} & -\frac{gx^*}{x^* + b} \\ \frac{hy^{*2}}{(x^* + c)^2} & 1 - \frac{r_2 y^{*2}}{(y^* + m_f)^2} \end{pmatrix}. \tag{21}$$

Let us assume that the matrix J_{E^*} has eigenvalues.

$$\begin{aligned}
\lambda_1 &= -1, \lambda_2 \\
&= 1 - ax^* + \frac{gx^* y^*}{(x^* + b)^2} + \frac{ghx^* y^{*2} (y^* + m_f)^2}{(x^* + b)(x^* + c)^2 (2(y^* + m_f)^2 - r_2 y^*)},
\end{aligned} \tag{22}$$

satisfies $|\lambda_1| = 1$ and $|\lambda_2| \neq 1$.

Next, we construct the nonsingular matrix L as follows:

$$L = \begin{pmatrix} \alpha_2 & \alpha_2 \\ -1 - \alpha_1 & \lambda_2 - \alpha_1 \end{pmatrix}. \tag{23}$$

Using translation $\begin{pmatrix} P_n \\ q_n \end{pmatrix} = L \begin{pmatrix} P_n \\ Q_n \end{pmatrix}$. Then, (17) can be written as

$$\begin{cases} P_{n+1} = -P_n + G_1(p_n, q_n, m_1) + o\left(\left(|p_n| + |q_n| + |m_1|\right)^2\right), \\ Q_{n+1} = \lambda_2 Q_n + G_2(p_n, q_n, m_1) + o\left(\left(|p_n| + |q_n| + |m_1|\right)^2\right), \end{cases} \quad (24)$$

where

$$\begin{aligned} G_1(p_n, q_n, m_1) &= \phi_1 m_1 + \phi_2 p_n^2 + \phi_3 q_n^2 + \phi_4 m_1^2 + \phi_5 p_n q_n + \phi_6 p_n m_1 + \phi_7 q_n m_1, \\ G_2(p_n, q_n, m_1) &= \theta_1 m_1 + \theta_2 p_n^2 + \theta_3 q_n^2 + \theta_4 m_1^2 + \theta_5 p_n q_n + \theta_6 p_n m_1 + \theta_7 q_n m_1, \end{aligned} \quad (25)$$

and

$$\begin{aligned} \phi_1 &= \frac{(\lambda_2 - \alpha_1)\alpha_3 - \alpha_2\beta_3}{\alpha_2(1 + \lambda_2)}, \\ \phi_2 &= \frac{(\lambda_2 - \alpha_1)\alpha_4 - \alpha_2\beta_4}{\alpha_2(1 + \lambda_2)}, \\ \phi_3 &= \frac{(\lambda_2 - \alpha_1)\alpha_5 - \alpha_2\beta_5}{\alpha_2(1 + \lambda_2)}, \\ \phi_4 &= \frac{(\lambda_2 - \alpha_1)\alpha_6 - \alpha_2\beta_6}{\alpha_2(1 + \lambda_2)} (1 + \lambda_2), \\ \phi_5 &= \frac{(\lambda_2 - \alpha_1)\alpha_7 - \alpha_2\beta_7}{\alpha_2(1 + \lambda_2)}, \\ \phi_6 &= \frac{(\lambda_2 - \alpha_1)\alpha_8 - \alpha_2\beta_8}{\alpha_2(1 + \lambda_2)}, \\ \phi_7 &= \frac{(\lambda_2 - \alpha_1)\alpha_9 - \alpha_2\beta_9}{\alpha_2(1 + \lambda_2)}, \\ \theta_1 &= \frac{(1 + \alpha_1)\alpha_3 + \alpha_2\beta_3}{\alpha_2(1 + \lambda_2)}, \\ \theta_2 &= \frac{(1 + \alpha_1)\alpha_4 + \alpha_2\beta_4}{\alpha_2(1 + \lambda_2)}, \\ \theta_3 &= \frac{(1 + \alpha_1)\alpha_5 + \alpha_2\beta_5}{\alpha_2(1 + \lambda_2)}, \\ \theta_4 &= \frac{(1 + \alpha_1)\alpha_6 + \alpha_2\beta_6}{\alpha_2(1 + \lambda_2)}, \\ \theta_5 &= \frac{(1 + \alpha_1)\alpha_7 + \alpha_2\beta_7}{\alpha_2(1 + \lambda_2)}, \\ \theta_6 &= \frac{(1 + \alpha_1)\alpha_8 + \alpha_2\beta_8}{\alpha_2(1 + \lambda_2)}, \\ \theta_7 &= \frac{(1 + \alpha_1)\alpha_9 + \alpha_2\beta_9}{\alpha_2(1 + \lambda_2)}. \end{aligned} \quad (26)$$

Now, by the center manifold theorem, we obtain the center manifold $G^c(0, 0)$ of system (19) at $(0, 0)$ in a small neighborhood of $m_1 = 0$ as follows:

$$\begin{aligned} G^c(0, 0) &= \{(P_n, Q_n): Q_n = h(P_n, m_1)\}, \\ &= \{(P_n, Q_n): Q_n = e_1 m_1 + e_2 P_n^2 + e_3 m_1 P_n \\ &\quad + e_4 m_1^2 + o\left(\left(|P_n| + |m_1|\right)^2\right)\}. \end{aligned} \quad (27)$$

On applying map (19) on both sides of $Q_n = h(P_n, m_1)$, we have the following:

$$\begin{aligned} \lambda_2 Q_n + G_2(p_n, q_n, m_1) &= e_1 m_1 + e_2 (-P_n + G_1(p_n, q_n, m_1))^2 \\ &\quad + e_3 m_1 (-P_n + G_1(p_n, q_n, m_1)) \\ &\quad + e_4 m_1^2 + o\left(\left(|P_n| + |m_1|\right)^2\right), \end{aligned} \quad (28)$$

where

$$\begin{aligned} p_n &= \alpha_2 (P_n + Q_n) = \alpha_2 (P_n + h(P_n, m_1)), \\ q_n &= (-1 - \alpha_1) P_n + (\lambda_2 - \alpha_1) Q_n \\ &= (-1 - \alpha_1) P_n + (\lambda_2 - \alpha_1) h(P_n, m_1), \\ e_1 &= \frac{\theta_1}{1 - \lambda_2}, \\ e_2 &= \frac{1}{1 - \lambda_2} [\theta_2 \alpha_2^2 + \theta_3 (1 + \alpha_1)^2 - \theta_5 \alpha_2 (-1 - \alpha_1)], \\ e_3 &= \frac{1}{1 + \lambda_2} [-2e_2 \phi_1 - \theta_6 \alpha_2 + \theta_7 (-1 - \alpha_1) - 2e_1 \theta_2 \alpha_2^2 \\ &\quad + 2e_1 \theta_3 (-1 - \alpha_1) (\lambda_2 - \alpha_1) - e_1 \theta_5 \alpha_2 (\beta_2 - \alpha_1)], \\ e_4 &= \frac{1}{1 - \lambda_2} [e_1^2 \theta_2 \alpha_2^2 + e_1^2 \theta_3 (\lambda_2 - \alpha_1)^2 + e_1^2 \theta_5 \alpha_2 (\lambda_2 - \alpha_1) \\ &\quad + e_1 \theta_6 \alpha_2 + e_1 \theta_7 (\lambda_2 - \alpha_1) - e_2 \phi_1^2 + \theta_4 - \phi_1 e_3]. \end{aligned} \quad (29)$$

Therefore, on the center manifold M^c at origin, we have where the following:

$$\begin{aligned} p_n^2 &= \beta_2^2(P_n^2 + 2P_nQ_n + Q_n^2), \\ p_nq_n &= -\beta_2(1 + \beta_1)P_n^2 + \beta_2(\delta_2 - \beta_1)P_nQ_n + \beta_2(\lambda_2 - \beta_1)Q_n^2, \\ q_n^2 &= (1 + \beta_1)^2P_n^2 - 2(1 + \beta_1)(\lambda_2 - \beta_1)P_nQ_n + (\lambda_2 - \beta_1)^2Q_n^2, \end{aligned} \quad (30)$$

$$\begin{aligned} P_nQ_n &= e_1m_1P_n + e_2P_n^3 + e_3m_1P_n^2 + e_4m_1^2P_n + o\left(\left(|P_n| + |m_1|\right)\right)^3, \\ Q_n^2 &= e_1^2m_1^2 + 2e_1e_2m_1P_n^2 + 2e_1e_3m_1^2P_n + 2e_1e_4m_1^3 + o\left(\left(|P_n| + |m_1|\right)\right)^3. \end{aligned} \quad (31)$$

Moreover, the map G^* restricted to CM $G^c(0,0)$ is as follows: where

$$\begin{aligned} G^*(P_n) &= -P_n + G_1(p_n, q_n, m_1) \\ &= -P_n + g_1m_1 + g_2P_n^2 + g_3P_nm_1 + g_4m_1^2 + g_5P_n^2m_1 \\ &\quad + g_6P_nm_1^2 + g_7P_n^3 + g_8m_1^3 + o\left(\left(|P_n| + |m_1|\right)\right)^3, \end{aligned} \quad (32)$$

$$\begin{aligned} g_1 &= \phi_1, \\ g_2 &= \phi_2\beta_2^2 + \phi_3(1 + \beta_1)^2 - \phi_5\beta_2(1 + \beta_1), \\ g_3 &= 2e_1\phi_2\beta_2^2 - 2e_1\phi_3(1 + \beta_1)(\lambda_2 - \beta_1) + e_1\phi_5\beta_2(\lambda_2 - \beta_1) + \phi_6\beta_2 - \phi_7(1 + \beta_1), \\ g_4 &= e_1^2\phi_2\beta_2^2 + e_1^2\phi_3(\lambda_2 - \beta_1)^2 + \phi_4 + e_1^2\phi_5\beta_2(\lambda_2 - \beta_1) + e_1\phi_6\beta_2 + e_1\phi_7(\lambda_2 - \beta_1), \\ g_5 &= 2e_3\phi_2\beta_2^2 + 2e_1e_2\phi_2\beta_2^2 - 2e_3\phi_3(1 + \beta_1)(\lambda_2 - \beta_1) + 2e_1e_2\phi_3(\lambda_2 - \beta_1)^2 + e_3\phi_5\beta_2 \\ &\quad (\lambda_2 - \beta_1) + 2e_1e_2\phi_5\beta_2(\lambda_2 - \beta_1) + e_2\phi_6\beta_2 + e_2\phi_7(\lambda_2 - \beta_1), \\ g_6 &= 2e_4\phi_2\beta_2^2 + 2e_1e_3\phi_2\beta_2^2 - 2e_4\phi_3(1 + \beta_1)(\lambda_2 - \beta_1) + 2e_1e_3\phi_3(\lambda_2 - \beta_1)^2 + e_4\phi_5\beta_2 \\ &\quad (\lambda_2 - \beta_1) + 2e_1e_3\phi_5\beta_2(\lambda_2 - \beta_1) + e_3\phi_6\beta_2 + e_3\phi_7(\lambda_2 - \beta_1), \\ g_7 &= 2e_2\phi_2\beta_2^2 - 2e_2\phi_3(1 + \beta_1)(\lambda_2 - \beta_1) + e_2\phi_5\beta_2(\lambda_2 - \beta_1), \\ g_8 &= 2e_1e_4\phi_2\beta_2^2 + 2e_1e_4\phi_3(\lambda_2 - \beta_1)^2 + 2e_1e_4\phi_5\beta_2(\lambda_2 - \beta_1) + e_4\phi_6\beta_2 + e_4\phi_7(\lambda_2 - \beta_1). \end{aligned} \quad (33)$$

From [43], we define ζ_1 and ζ_2 as follows:

$$\zeta_1 = \left(G_{P_n, m_1}^* + \frac{1}{2} G_{m_1}^* G_{P_n, P_n}^* \right) \Big|_{(P_n, m_1) = (0,0)} = g_3 + g_1g_2, \quad (34)$$

$$\zeta_2 = \left(\frac{1}{6} G_{P_n, P_n, P_n}^* + \left(\frac{1}{2} G_{P_n, P_n}^* \right)^2 \right) \Big|_{(P_n, m_1) = (0,0)} = g_7 + g_2^2. \quad (35)$$

Therefore, we have got the following findings of flip bifurcation from the aforementioned study.

Theorem 1. *If $\zeta_1 \neq 0$ and $\zeta_2 \neq 0$, then system (5) exhibits a flip bifurcation at $E^*(x^*, y^*)$ when m_1 changes in a small neighborhood of the origin. Moreover, if $\zeta_2 > 0$ (or $\zeta_2 < 0$), then the existing period-two orbits from $E^*(x^*, y^*)$ are stable (or unstable).*

4.2. Neimark–Sacker Bifurcation. In this subsection, we find the condition for the existence of Neimark–Sacker (NS) bifurcation and also its direction and stability properties for system (5) near $E^*(x^*, y^*)$ using the method followed in [32, 42]. For the existence of NS bifurcation of system (5), the complex conjugate eigenvalues of the characteristic

equation at $E^*(x^*, y^*)$ should have absolute value one. For this, it is necessary to satisfy the following:

$$(B_1(x^*, y^*))^2 - 4B_2(x^*, y^*) < 0 \text{ and } B_2(x^*, y^*) = 1, \quad (36)$$

which provides

$$\begin{aligned} A(m) &:= \left(2 - ax^* + \frac{gx^*y^*}{(x^*+b)^2} - \frac{r_2y^{*2}}{(y^*+m)^2} \right)^2 - 4 \left(1 - ax^* + \frac{gx^*y^*}{(x^*+b)^2} \right) \\ &\quad - \frac{r_2(1-ax^*)y^{*2}}{(y^*+m)^2} - \frac{gr_2x^*y^{*3}}{(x^*+b)^2(y^*+m)^2} + \frac{ghx^*y^{*2}}{(x^*+b)(x^*+c)^2} < 0, \\ B(m) &:= -ax^* + \frac{gx^*y^*}{(x^*+b)^2} - \frac{r_2(1-ax^*)y^{*2}}{(y^*+m)^2} - \frac{gr_2x^*y^{*3}}{(x^*+b)^2(y^*+m)^2} + \frac{ghx^*y^{*2}}{(x^*+b)^2(x^*+c)^2} = 0. \end{aligned} \quad (37)$$

Note that the left-hand side of (37) is in terms of m since m is taken as a bifurcation parameter. It is difficult to find the explicit expression for the critical value m to satisfy (24) for the occurrence of NS bifurcation of system (5). Therefore, we assume that the critical value is $m = m_h$. Also, the interior equilibrium $E^*(x^*, y^*)$ is calculated at the critical value $m = m_h$.

Next, if $a_2 > 0$, $a_3 < 0$, and $h(y^* + m)/r_2 > c$ holds, we define the neighborhood as follows:

$$\Theta_h = \{(r_1, r_2, a, b, c, g, h, m) : m = m_h, r_1, r_2, a, b, c, g, h > 0\}. \quad (38)$$

Then, the equilibrium point $E^*(x^*, y^*)$ can arise NS bifurcation at $m = m_h$ when it changes in the neighborhood

of Θ_h . Now, we analyze the properties of possible NS bifurcation at $E^*(x^*, y^*)$ for system (5) if (24) holds for some m_h . Given a perturbation $|m_2| \ll 1$ of critical value m_h , then the perturbation system is described as follows:

$$\begin{cases} x_{n+1} = x_n \exp \left[r_1 - ax_n - \frac{gy_n}{x_n + b} \right], \\ y_{n+1} = y_n \exp \left[\frac{r_2y_n}{y_n + (m_2 + m_h)} - \frac{hy_n}{x_n + c} \right]. \end{cases} \quad (39)$$

Let us use the transform $p_n = x_n - x^*$, $q_n = y_n - y^*$ and shift $E^*(x^*, y^*)$ to $(0, 0)$. Then, system (28) takes the following form:

$$\begin{cases} p_{n+1} = (p_n + x^*) \exp \left[r_1 - a(p_n + x^*) - \frac{g(q_n + y^*)}{E^*(x^*, y^*) + b} \right] - x^*, \\ q_{n+1} = (q_n + y^*) \exp \left[\frac{r_2(q_n + y^*)}{(q_n + y^*) + (m_2 + m_h)} - \frac{h(q_n + y^*)}{E^*(x^*, y^*) + c} \right] - y^*. \end{cases} \quad (40)$$

Therefore, by Taylor expansion of (40),

$$\begin{cases} p_{n+1} = \rho_1 p_n + \rho_2 q_n + \rho_3 p_n^2 + \rho_4 p_n q_n + \rho_5 q_n^2 + \rho_6 p_n^3 \\ \quad + \rho_7 p_n^2 q_n + \rho_8 p_n v_n^2 + \rho_9 v_n^3 + o\left(\left(|p_n| + |q_n|\right)^3\right), \\ q_{n+1} = \eta_1 p_n + \eta_2 q_n + \eta_3 p_n^2 + \eta_4 p_n q_n + \eta_5 q_n^2 + \eta_6 p_n^3 + \eta_7 p_n^2 q_n \\ \quad + \eta_8 p_n v_n^2 + \eta_9 v_n^3 + o\left(\left(|p_n| + |q_n|\right)^3\right), \end{cases} \quad (41)$$

where

$$\begin{aligned}
\rho_1 &= 1 + x^* N_1, \\
\rho_2 &= \frac{-gx^*}{x^* + b}, \\
\rho_3 &= \frac{-gx^* y^*}{(x^* + b)^3} + N_1 + \frac{x^* N_1^2}{2}, \\
\rho_4 &= -\frac{gb}{(x^* + b)^2} - \frac{gN_1 x^*}{x^* + b}, \\
\rho_5 &= \frac{g^2 x^*}{2(x^* + b)^2}, \\
\rho_6 &= -\frac{bgy^*}{(x^* + b)^4} - \frac{gN_1 x^* y^*}{(x^* + b)^3} + \frac{N_1^2}{2} + \frac{x^* N_1^3}{6}, \\
\rho_7 &= \frac{g^2 x^* y^*}{(x^* + b)^4} + \frac{gb}{(x^* + b)^3} - \frac{gbN_1}{(x^* + b)^2} - \frac{gN_1^2 x^*}{2(x^* + b)}, \\
\rho_8 &= -\frac{g^2 x^*}{(x^* + b)^3} + \frac{g^2(1 + x^* N_1)}{2(x^* + b)^2}, \\
\rho_9 &= -\frac{g^3 x^*}{6(x^* + b)^3}, \\
\eta_1 &= \frac{hy^{*2}}{(x^* + c)^2}, \\
\eta_2 &= 1 + y^* N_2, \\
\eta_3 &= \frac{-hy^{*2}}{(x^* + c)^3} + \frac{h^2 y^{*3}}{2(x^* + c)^4}, \\
\eta_4 &= \frac{2hy^*}{(x^* + c)^2} + \frac{hy^{*2} N_2}{(x^* + c)^2}, \\
\eta_5 &= \frac{-r_2 m_h y^*}{(y^* + m_h)^3} + N_2 + \frac{y^* N_2^2}{2}, \\
\eta_6 &= \frac{hy^{*2}}{(x^* + c)^4} - \frac{h^2 y^{*3}}{(x^* + c)^5} + \frac{h^3 y^{*4}}{6(x^* + c)^6}, \\
\eta_7 &= \frac{-hy^*(2 + y^* N_2)}{(x^* + c)^3} + \frac{h^2 y^{*2}(3 + y^* N_2)}{2(x^* + c)^4}, \\
\eta_8 &= \frac{h(1 + y^{*2} N_2^2)}{2(x^* + c)^2} + \frac{2hy^* N_2}{(x^* + c)^2} - \frac{r_2 m_h}{(y^* + m_h)^2}, \\
\eta_9 &= \frac{r_2 m_h y^*}{(y^* + m_h)^4} - \frac{r_2 m_h(1 + N_2 y^*)}{(y^* + m_h)^3} + \frac{N_2^2}{2} + \frac{N_2^3 y^*}{6}, \\
N_1 &= -a + \frac{gy^*}{(x^* + b)^2}, \\
N_2 &= \frac{-r_2 y^*}{(y^* + m_h)^2}.
\end{aligned} \tag{42}$$

The characteristic polynomial equation associated with the linearized system (30) at the origin can be given as follows:

$$\lambda^2 + q_1(m_2)\lambda + q_2(m_2) = 0, \tag{43}$$

where

$$\begin{aligned}
q_1(m_2) &= \left(-1 + ax^* - \frac{gx^* y^*}{(x^* + b)^2} \right) \Omega_1 \\
&\quad - \left(1 - \frac{r_2 y^{*2}}{(y^* + (m_h + m_2))^2} \right) \Omega_2, \\
q_2(m_2) &= \left[\left(1 - ax^* + \frac{gx^* y^*}{(x^* + b)^2} \right) \left(1 - \frac{r_2 y^{*2}}{(y^* + (m_h + m_2))^2} \right) \right. \\
&\quad \left. + \frac{ghx^* y^{*2}}{(x^* + b)(x^* + c)^2} \right] \Omega_1 \Omega_2,
\end{aligned} \tag{44}$$

With $\Omega_1 = \exp[r_1 - ax^* - gy^*/x^* + b]$ and $\Omega_2 = \exp[r_2 y^*/y^* + (m_h + m_2) - hy^*/x^* + c]$. Now, the roots of (43) are the pair of complex conjugates.

$$\lambda_{1,2} = \frac{1}{2} \left[-q_1(m_2) \pm i \sqrt{4q_2(m_2) - (q_1(m_2))^2} \right]. \tag{45}$$

Since $(r_1, r_2, a, b, c, g, h, m) \in \Theta_h$, we have,
 $|\lambda_{1,2}| = \sqrt{q_2(m_2)}$
and

$$\begin{aligned}
\frac{d|\lambda_{1,2}|}{dm_2} &= \frac{1}{2\sqrt{q_2(0)}} \left\{ \left(1 - ax^* + \frac{gx^* y^*}{(x^* + b)^2} \right) \left(\frac{2r_2 y^{*2}}{(y^* + m_h)^3} \right) \right. \\
&\quad \left. - \frac{r_2 y^*}{(y^* + m_h)^2} \left[\left(1 - ax^* + \frac{gx^* y^*}{(x^* + b)^2} \right) \right] \right. \\
&\quad \left. \times \left(1 - \frac{r_2 y^{*2}}{(y^* + m_h)^2} \right) + \frac{ghx^* y^{*2}}{(x^* + b)(x^* + c)^2} \right\} \neq 0.
\end{aligned} \tag{46}$$

Furthermore, it is required $\lambda_1^k, \lambda_2^k \neq 1$ for $k = 1, 2, 3, 4$, when $m_2 = 0$, which implies $q_1(0) = \pm 2, 0, -1$. Therefore, $q_1(0) = -2 + ax^* - gx^* y^*/(x^* + b)^2 + r_2 y^{*2}/(y^* + m_h)^2 \neq \pm 2$. We only require $q_1(0) \neq 0, 1$, i.e.,

$$ax^* - \frac{gx^* y^*}{(x^* + b)^2} + \frac{r_2 y^{*2}}{(y^* + m_h)^2} \neq 2, 3. \tag{47}$$

Let $m_2 = 0$, $\sigma = -q_1(0)/2$, and $\theta = \sqrt{4q_2(0) - q_1^2(0)}/2$, and construct the nonsingular matrix.

$$L = \begin{pmatrix} \rho_2 & 0 \\ \sigma - \rho_1 & \theta \end{pmatrix}, \tag{48}$$

Use the translation $\begin{pmatrix} P_n \\ Q_n \end{pmatrix} = L \begin{pmatrix} P_n \\ Q_n \end{pmatrix}$. Thus, system (30) where takes the following form:

$$\begin{cases} P_{n+1} = \sigma P_n + \theta Q_n + R_1(P_n, Q_n) + o\left(\left(|P_n| + |Q_n|\right)^3\right), \\ Q_{n+1} = -\theta P_n + \sigma Q_n + R_2(P_n, Q_n) + o\left(\left(|P_n| + |Q_n|\right)^3\right), \end{cases} \quad (49)$$

$$R_1(P_n, Q_n) = \frac{1}{\rho_2} \begin{bmatrix} \{\rho_3 \rho_2^2 + \rho_4 \rho_2 (\sigma - \rho_1) + \rho_5 (\sigma - \rho_1)^2\} P_n^2 \\ + \{\rho_4 \rho_2 \theta + 2\theta \rho_5 (\sigma - \rho_1)\} P_n Q_n + \rho_5 \theta^2 Q_n^2 \\ + \{\rho_6 \rho_2^3 + \rho_7 \rho_2^2 (\sigma - \rho_1) + \rho_8 \rho_2 (\sigma - \rho_1)^2 + \rho_9 (\sigma - \rho_1)^3\} P_n^3 \\ + \{\rho_7 \rho_2^2 + 2\theta \rho_8 \rho_2 (\sigma - \rho_1) + 3\theta \rho_9 (\sigma - \rho_1) (\sigma - \rho_1)^2\} P_n^2 Q_n \\ + \{\theta^2 \rho_8 \rho_2 + 3\theta^2 \rho_9 (\sigma - \rho_1)\} P_n Q_n^2 + \theta^3 \rho_9 Q_n^3 \end{bmatrix},$$

$$R_2(P_n, Q_n) = \begin{bmatrix} \frac{1}{\rho_2 \theta} \{\rho_2^2 \rho_3 (\rho_1 - \sigma) + \rho_2 \eta_3 + \rho_2 (\sigma - \rho_1) (\rho_4 (\rho_1 - \sigma) \\ + \rho_2 \eta_4) + (\sigma - \rho_1)^2 (\rho_5 (\rho_1 - \sigma) + \rho_2 \eta_5)\} P_n^2 + \{\theta \rho_2 (\rho_4 \\ \times (\rho_1 - \sigma) + \rho_2 \eta_4) + 2\theta (\sigma - \rho_1) (\rho_5 (\rho_1 - \sigma) + \rho_2 \eta_5)\} P_n Q_n \\ + \theta^2 \{\rho_5 (\rho_1 - \sigma) + \rho_2 \eta_5\} Q_n^2 + \{\rho_2^3 \rho ((\rho_1 - \sigma) + \rho_2 \eta_6) \\ + \rho_2^2 (\sigma - \rho_1) (\rho_7 (\rho_1 - \sigma) + \rho_2 \eta_7) + \rho_2 (\sigma - \rho_1)^2 (\rho_8 (\rho_1 - \sigma) \\ + \rho_2 \eta_8) (\sigma - \rho_1)^3 (\rho_9 (\rho_1 - \sigma) + \rho_2 \eta_9)\} P_n^3 + \{\theta \rho_2^2 (\rho_7 (\rho_1 - \sigma) \\ + \rho_2 \eta_7) + 2\theta \rho_2 (\sigma - \rho_1) (\rho_8 (\rho_1 - \sigma) + \rho_2 \eta_8) + 3\theta (\sigma - \rho_1)^2 \\ \times (\rho_9 (\rho_1 - \sigma) + \rho_2 \eta_9)\} P_n^2 Q_n + \{\theta^2 \rho_2 (\rho_8 (\rho_1 - \sigma) + \rho_2 \eta_8) \\ + 3\theta^2 (\sigma - \rho_1) (\rho_9 (\rho_1 - \sigma) + \rho_2 \eta_9)\} P_n Q_n^2 + \theta^3 (\rho_9 (\rho_1 - \sigma) \\ + \rho_2 \eta_9) Q_n^3. \end{bmatrix} \quad (50)$$

Next, we require the nonzero quantity χ^* to ensure that system (34) undergoes NS bifurcation.

$$\chi^* = -\text{Re} \left[\frac{(1-2\lambda)\bar{\lambda}^2}{1-\lambda} \xi_{11} \xi_{20} \right] - \frac{1}{2} |\xi_{11}|^2 - |\xi_{02}|^2 + \text{Re}(\bar{\lambda} \xi_{21}), \quad (51)$$

where

$$\begin{aligned}\xi_{20} &= \frac{1}{8} \left[(R_{1P_n P_n} - R_{1Q_n Q_n} + 2R_{2P_n Q_n}) + i(R_{2P_n P_n} - R_{2Q_n Q_n} - 2R_{1P_n Q_n}) \right], \\ \xi_{11} &= \frac{1}{4} \left[(R_{1P_n P_n} + R_{1Q_n Q_n}) + i(R_{2P_n P_n} + R_{2Q_n Q_n}) \right], \\ \xi_{02} &= \frac{1}{8} \left[(R_{1P_n P_n} - R_{1Q_n Q_n} - 2R_{2P_n Q_n}) + i(R_{2P_n P_n} - R_{2Q_n Q_n} + 2R_{1P_n Q_n}) \right], \\ \xi_{21} &= \frac{1}{16} \left[\begin{aligned} &(R_{1P_n P_n P_n} + R_{1P_n Q_n Q_n} + R_{2P_n P_n Q_n} + R_{2Q_n Q_n Q_n}) \\ &+ i(R_{2P_n P_n P_n} + R_{2P_n Q_n Q_n} - R_{1P_n P_n Q_n} - R_{1Q_n Q_n Q_n}) \end{aligned} \right].\end{aligned}\quad (52)$$

Therefore, from [42], we can state the subsequent results.

Theorem 2. *If (32) and (33) hold and also the quantity χ^* is nonzero, then system (28) admits NS bifurcation at $E^*(x^*, y^*)$ when m_h changes in the neighborhood of Θ_h . Additionally, if the quantity $\chi^* < 0$ (or $\chi^* > 0$), then the stable (or unstable) invariant closed curve starts to bifurcate from $E^*(x^*, y^*)$.*

5. Chaos Control

In this section, we study the chaos control analyses for system (5). Firstly, we use the state feedback control method as in [27] to control the chaotic system. For system (5), we consider the following corresponding controlled system:

$$\begin{cases} x_{n+1} = x_n \exp \left[r_1 - ax_n - \frac{gy_n}{x_n + b} - u(x_n, y_n) \right], \\ y_{n+1} = y_n \exp \left[\frac{r_2 y_n}{y_n + m} - \frac{hy_n}{x_n + c} \right], \end{cases} \quad (53)$$

where $u(x_n, y_n) = h_1(x_n - x^*) + h_2(y_n - y^*)$ is the feedback controlling force with feedback gains h_1 and h_2 , with equilibrium $E^*(x^*, y^*)$ of (53). For the controlled system (36), the Jacobian matrix at $E^*(x^*, y^*)$ is given as

$$J(x^*, y^*) = \begin{pmatrix} \kappa_{11} - h_1 & \kappa_{12} - h_2 \\ \kappa_{21} & \kappa_{22} \end{pmatrix}, \quad (54)$$

where

$$\begin{aligned}\kappa_{11} &= 1 - ax^* + \frac{gx^* y^*}{(x^* + b)^2}, \\ \kappa_{12} &= -\frac{gx^*}{x^* + b}, \\ \kappa_{21} &= \frac{hy^{*2}}{(x^* + b)^2}, \\ \kappa_{22} &= 1 - \frac{r_2 y^{*2}}{(y^* + m)^2}.\end{aligned}\quad (55)$$

Then, for $J(x^*, y^*)$, we have the characteristic equation as follows:

$$\bar{\lambda}^2 - (\kappa_{11} + \kappa_{22} - h_1)\bar{\lambda} + \kappa_{22}(\kappa_{11} - h_1) - \kappa_{21}(\kappa_{12} - h_2) = 0. \quad (56)$$

Let $\bar{\lambda}_1$ and $\bar{\lambda}_2$ be the eigenvalues of (54), which yields the following:

$$\bar{\lambda}_1 + \bar{\lambda}_2 = \kappa_{11} + \kappa_{22} - h_1, \quad (57)$$

$$\bar{\lambda}_1 \bar{\lambda}_2 = \kappa_{22}(\kappa_{11} - h_1) - \kappa_{21}(\kappa_{12} - h_2). \quad (58)$$

Using (57) and (58), $\bar{\lambda}_1 \bar{\lambda}_2 = 1$, $\bar{\lambda}_1 = 1$, and $\bar{\lambda}_1 = -1$. Also, ensure that $|\bar{\lambda}_{1,2}| < 1$. Then, we derive the marginal stability lines as follows:

$$\begin{aligned}\bar{L}_1: & \kappa_{11}\kappa_{22} - \kappa_{21}\kappa_{12} - 1 = h_1\kappa_{22} - h_2\kappa_{21}, \\ \bar{L}_2: & h_1(1 - \kappa_{22}) + h_2\kappa_{21} = \kappa_{11} + \kappa_{22} - 1 - \kappa_{11}\kappa_{22} + \kappa_{21}\kappa_{12}, \\ \bar{L}_3: & h_1(1 + \kappa_{22}) - h_2\kappa_{21} = \kappa_{11} + \kappa_{22} + 1 + \kappa_{11}\kappa_{22} - \kappa_{21}\kappa_{12}.\end{aligned}\quad (59)$$

Moreover, the triangular region enclosed by lines \bar{L}_1 , \bar{L}_2 , and \bar{L}_3 have stable eigenvalues for the Jacobian matrix (37).

Next, the pole-placement control method, as in [31], is utilized to control the unstable dynamics of system (5). By taking m as control parameter, we rewrite system (5) as follows:

$$\begin{cases} x_{n+1} = x_n \exp \left[r_1 - ax_n - \frac{gy_n}{x_n + b} \right] = f_1(x_n, y_n), \\ y_{n+1} = y_n \exp \left[\frac{r_2 y_n}{y_n + m} - \frac{hy_n}{x_n + c} \right] = f_2(x_n, y_n). \end{cases} \quad (60)$$

Furthermore, m is needed to lie in some interval $|m - m_0| < \delta$ with $\delta > 0$ and m_0 denotes the nominal value, for which system (5) has unstable dynamics. Now, we utilize the state feedback control method to shift the trajectory to the expected state. Let the equilibrium point $E^*(x^*, y^*)$ be unstable for system (5) because of NS bifurcation. Then,

system (5) can be approximated near $E^*(x^*, y^*)$ using the linear map, which is given by the following:

$$\begin{pmatrix} x_{n+1} - x^* \\ y_{n+1} - y^* \end{pmatrix} \approx A \begin{pmatrix} x_n - x^* \\ y_n - y^* \end{pmatrix} + tBn[m - m_0], \quad (61)$$

where

$$A = \begin{pmatrix} \frac{\partial f_1(x^*, y^*, m_0)}{\partial x_n} & \frac{\partial f_1(x^*, y^*, m_0)}{\partial y_n} \\ \frac{\partial f_2(x^*, y^*, m_0)}{\partial x_n} & \frac{\partial f_2(x^*, y^*, m_0)}{\partial y_n} \end{pmatrix},$$

$$B = \begin{pmatrix} \frac{\partial f_1(x^*, y^*, m_0)}{\partial m} \\ \frac{\partial f_2(x^*, y^*, m_0)}{\partial m} \end{pmatrix} \quad (62)$$

$$= \begin{pmatrix} 0 \\ \frac{-r_2 y^*}{(y^* + m)^2} \end{pmatrix}.$$

It is clear to observe that system (44) is controllable, provided matrix C has rank 2, which is,

$$C = (B: AB) = \begin{pmatrix} 0 & \left(\frac{\partial f_1(x^*, y^*, m_0)}{\partial y_n} \right) \frac{-r_2 y^{*2}}{(y^* + m)^2} \\ \frac{-r_2 y^*}{(y^* + m)^2} & \left(\frac{\partial f_2(x^*, y^*, m_0)}{\partial y_n} \right) \frac{-r_2 y^*}{(y^* + m)^2} \end{pmatrix}. \quad (63)$$

Furthermore, $-r_2 y^{*2}/(y^* + m)^2 \neq 0$, and assume that $\partial f_2(x^*, y^*, m_0)/\partial y_n \neq 0$. Then, system (44) is controllable.

Next, we assume that $[m - m_0] = -K \begin{bmatrix} x_n - x^* \\ y_n - y^* \end{bmatrix}$, where $K = [s_1 \ s_2]$. Then, system (44) can be written as follows:

$$\begin{pmatrix} x_{n+1} - x^* \\ y_{n+1} - y^* \end{pmatrix} \approx (A - BK) \begin{pmatrix} x_n - x^* \\ y_n - y^* \end{pmatrix}. \quad (64)$$

Then, the controller system is given by the following:

$$\begin{cases} x_{n+1} = x_n \exp \left[r_1 - ax_n - \frac{gy_n}{x_n + b} \right] = f_1(x_n, y_n), \\ y_{n+1} = y_n \exp \left[\frac{r_2 y_n}{m_0 - S + y_n} - \frac{hy_n}{x_n + c} \right] = f_2(x_n, y_n). \end{cases} \quad (65)$$

where $S = s_1(x_n - x^*) + s_2(y_n - y^*)$. Furthermore, if the matrix $A - BK$ has eigenvalues $\bar{\lambda}_1$ and $\bar{\lambda}_2$ that lie in an open

unit disk, then $E^*(x^*, y^*)$ is locally asymptotically stable. Thus, we have the following:

$$A - BK = \begin{pmatrix} \kappa_{11} & \kappa_{12} \\ \kappa_{21} - \theta s_1 & \kappa_{22} - \theta s_1 \end{pmatrix}, \quad (66)$$

where $\theta = -r_2 y^{*2}/(y^* + m)^2$, and κ_{11} , κ_{12} , κ_{21} , and κ_{22} are the same as in (54). Then, the characteristic polynomial of (66) can be written as follows:

$$\bar{\lambda}^2 - (\kappa_{11} + \kappa_{22} - \theta s_2)\bar{\lambda} + \kappa_{11}(\kappa_{22} - \theta s_2) + \kappa_{12}(\theta s_1 - \kappa_{21}) = 0. \quad (67)$$

The lines of marginal stability are obtained, which are as follows:

$$\begin{aligned} \bar{L}_1: & \kappa_{11}(\kappa_{22} - \theta s_2) + \kappa_{12}(\theta s_1 - \kappa_{21}) = 1, \\ \bar{L}_2: & \kappa_{11} + \kappa_{22} = 1 + \theta s_2 + \kappa_{11}(\kappa_{22} - \theta s_2) + \kappa_{12}(\theta s_1 - \kappa_{21}), \\ \bar{L}_3: & \theta s_2 = \kappa_{11} + \kappa_{22} + 1 + \kappa_{11}(\kappa_{22} - \theta s_2) + \kappa_{12}(\theta s_1 - \kappa_{21}). \end{aligned} \quad (68)$$

Therefore, matrix (49) has stable eigenvalues enclosed by the straight lines \bar{L}_1 , \bar{L}_2 , and \bar{L}_3 in s_1, s_2 - plane.

Next, we apply the hybrid control feedback methodology [28, 29] for controlling the bifurcation behavior of the system near the equilibrium point $E^*(x^*, y^*)$. Then, the controlled system can be written as follows:

$$\begin{cases} x_{n+1} = \epsilon x_n \exp \left[r_1 - ax_n - \frac{gy_n}{x_n + b} \right] + (1 - \epsilon)x_n, \\ y_{n+1} = \epsilon y_n \exp \left[\frac{r_2 y_n}{y_n + m} - \frac{hy_n}{x_n + c} \right] + (1 - \epsilon)y_n, \end{cases} \quad (69)$$

where $0 < \epsilon < 1$ is the controlled strategy of the combination of both feedback control and parameter perturbation. The Jacobian matrix evaluated for system (54) at $E^*(x^*, y^*)$ is given by the following:

$$\begin{pmatrix} 1 - \epsilon ax^* + \frac{\epsilon gx^* y^*}{(x^* + b)^2} & \frac{\epsilon gx^*}{x^* + b} \\ \frac{\epsilon hy^{*2}}{(x^* + c)^2} & 1 - \frac{\epsilon r_2 y^{*2}}{(y^* + m)^2} \end{pmatrix}. \quad (70)$$

Note that one can select the appropriate value for ϵ to ensure that all eigenvalues of the above matrix satisfy $|\bar{\lambda}_{1,2}| < 1$.

Remark 1. System (2) is the extension of a continuous-time system (1) with the Allee effect in the predator's growth term. It is worth mentioning here that the discrete form of system (2) is not studied elsewhere in the literature. Hence, we obtained discrete-time system (5) from (2) using methods similar to those in [11, 12]. Moreover, the influence of the Allee effect is shown in terms of flip and Neimark-Sacker

TABLE 1: The equilibrium point values of Case (i).

m	x^*	y^*
0.2	0.755 253	2.190 958
0.27	0.762 114	2.134 027
0.4	0.774 789	2.028 170
0.5	0.784 481	1.946 631
0.53	0.787 379	1.922 151
0.9	0.822 760	1.619 543

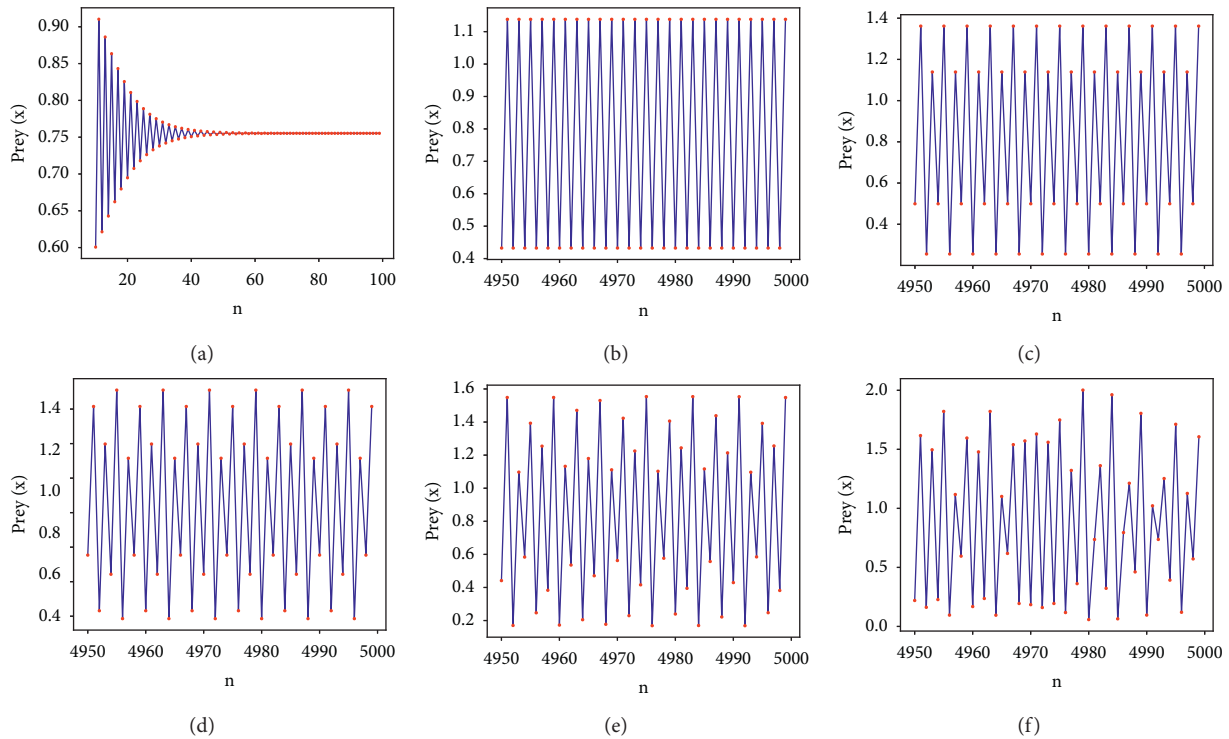


FIGURE 1: The time series plots for system (5) with $r_1 = 3.3$, $a = 3.3$, $g = 1.2$, $b = 2.5$, $r_2 = 1$, $h = 0.525$, and $c = 0.5$ (a) locally stable for $m = 0.2$, (b) period-2 for $m = 0.27$, (c) period-4 for $m = 0.4$, (d) period-8 for $m = 0.5$, (e) 8-chaotic like attractor for $m = 0.53$, and (f) chaotic attractor for $m = 0.9$.

bifurcations for system (5). Using the results in [42, 43], the direction and stability properties of both bifurcations can be discussed with the help of Theorem 1 and 2. Also, the bifurcation and chaos control analyses are carried out by utilizing the methods in [27–31].

6. Numerical Simulations

In the subsequent section, we perform some simulations for system (5) at $E^*(x^*, y^*)$ to ensure our mathematical results obtained in the previous sections.

Case (i): firstly, let us take the parameter values as $r_1 = 3.3$, $a = 3.3$, $g = 1.2$, $b = 2.5$, $r_2 = 1$, $h = 0.525$, and $c = 0.5$ and varying $m \in (0, 1]$ for system (5). Then, system (5) exhibits flip bifurcation when m reaches the critical value $m_f = 0.28805$, and the interior equilibrium point at m_f is $E^*(x^*, y^*) = (0.76387948, 2.11933949)$, which also satisfies (13). Also, the characteristic (12) is given by the following:

$$\lambda^2 + 1.11345044\lambda + 0.11345926 = 0, \quad (71)$$

where $\lambda_{1,2} = -0.11346, -1$ are the eigenvalues of the Jacobian matrix at $E^*(x^*, y^*)|_{m_f}$. Then, from (34) and (35), we obtain $\zeta_1 = 1.3842$ and $\zeta_2 = 5.17693$, and the properties of flip bifurcation are illustrated in Theorem 1.

The interior equilibrium point varies accordingly for various values of m , which is given in Table 1. The nature of system (5) near $E^*(x^*, y^*)$ is shown for different values of m , for $m = 0.2$ is stable, $m = 0.27$ is period-2, $m = 0.4$ is period-4, $m = 0.5$ is period-8, $m = 0.53$ is chaotic, and $m = 0.9$ is chaotic, which are shown by the time series plots in Figure 1 and the phase portraits in Figure 2. It shows that the system becomes chaotic from stable via period-doubling cascade for larger values of m . Also, the chaotic nature of the system is confirmed by one parameter bifurcation diagram and the maximum Lyapunov exponent in Figure 3.

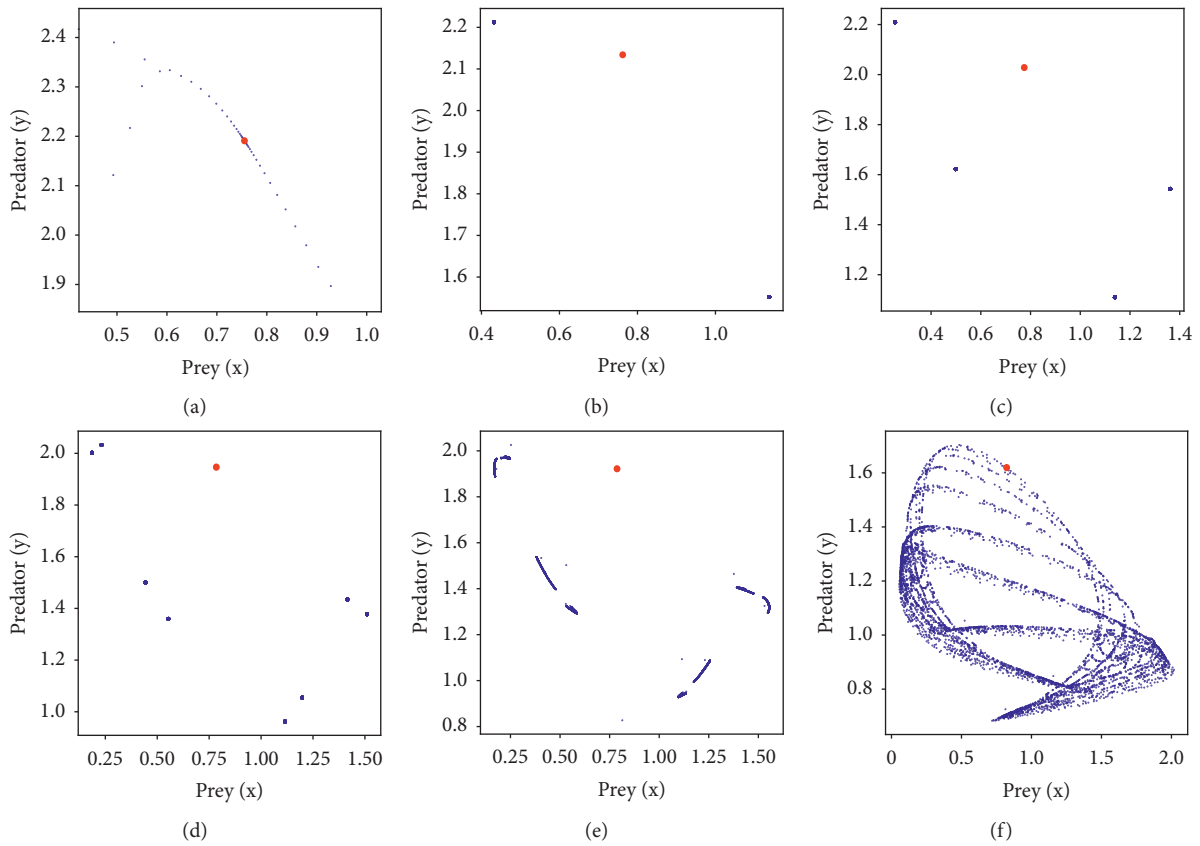


FIGURE 2: The phase portraits for system (5) with $r_1 = 3.3$, $a = 3.3$, $g = 1.2$, $b = 2.5$, $r_2 = 1$, $h = 0.525$, and $c = 0.5$ (a) locally stable for $m = 0.2$, (b) period-2 for $m = 0.27$, (c) period-4 for $m = 0.4$, (d) period-8 for $m = 0.5$, (e) 8-chaotic like attractor for $m = 0.53$, and (f) chaotic attractor for $m = 0.9$. The red points represent the interior equilibrium point $E^*(x^*, y^*)$, and its values are given in Table 1.

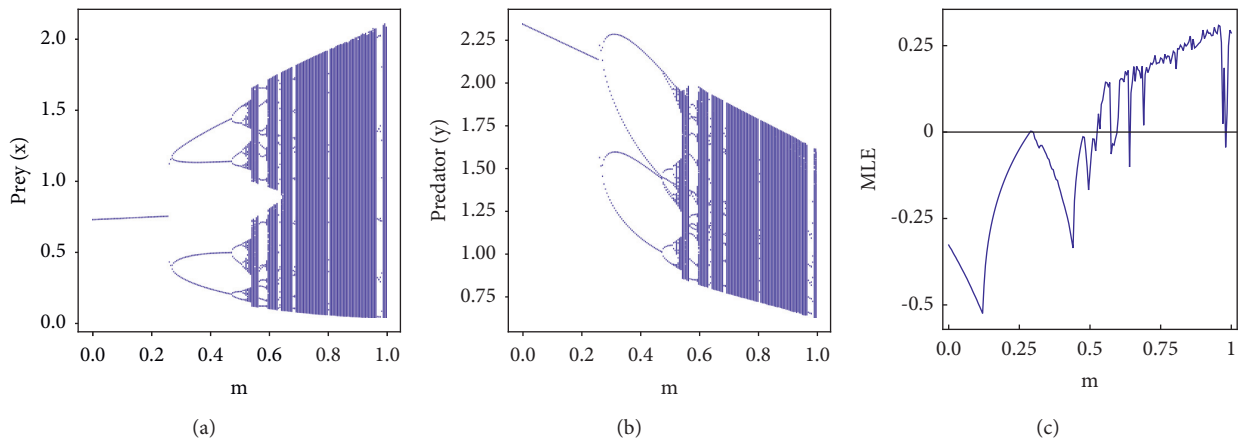


FIGURE 3: ((a), (b)). The flip bifurcation diagrams. (c) The maximum Lyapunov exponents for system (5) with $r_1 = 3.3$, $a = 3.3$, $g = 1.2$, $b = 2.5$, $r_2 = 1$, $h = 0.525$, $c = 0.5$, and $m \in [0, 1]$.

TABLE 2: The equilibrium point values of Case (ii).

m	x^*	y^*
0.18	0.655 489	2.230 839
0.2	0.692 054	2.245 334
0.5	1.099 589	2.329 801
0.58	1.184 178	2.329 602
0.88	1.457 370	2.287 330
0.9	1.513 887	2.270 648

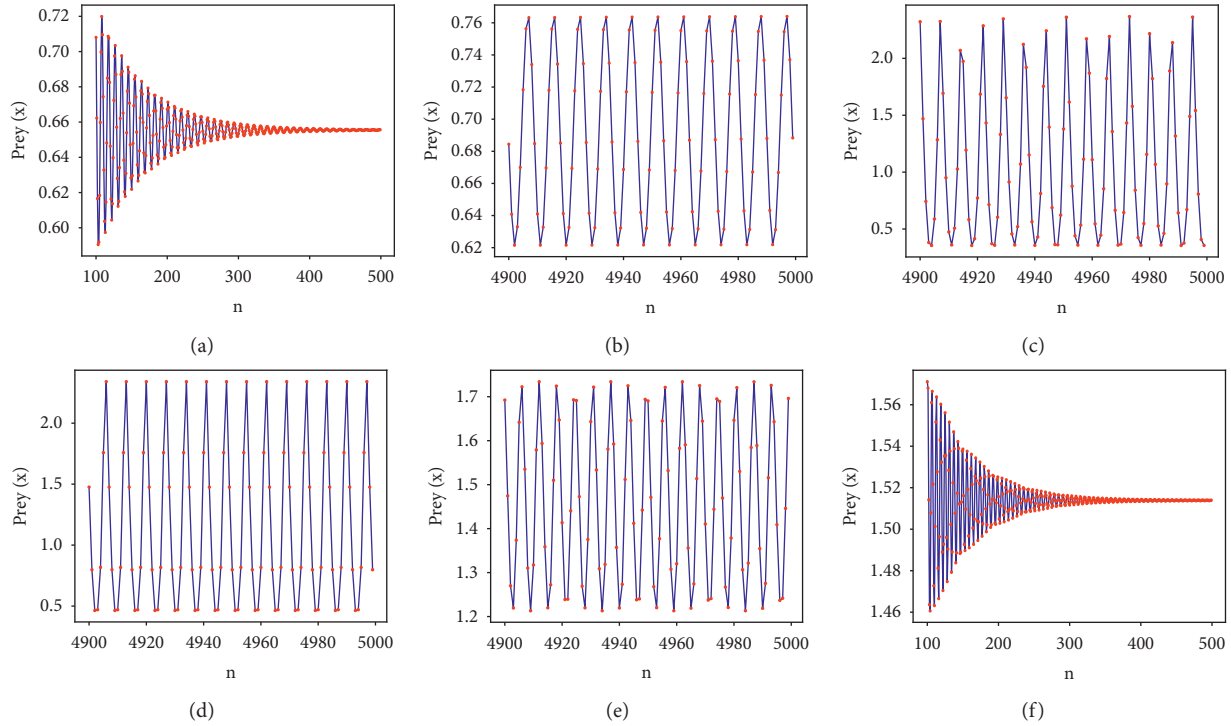


FIGURE 4: The time series plots for system (5) with $r_1 = 4, a = 1.15, g = 2.7, b = 1.2, r_2 = 1, h = 1.06,$ and $c = 1.9$ (a) asymptotically stable for $m = 0.18,$ ((b), (c)) invariant circles for $m = 0.2, 0.5,$ (d) period-8 for $m = 0.58,$ (e) invariant circle for $m = 0.88,$ and (e) asymptotically stable for $m = 0.95.$

Case (ii): next, choose the system parameter values as $r_1 = 4, a = 1.15, g = 2.7, b = 1.2, r_2 = 1, h = 1.06, c = 1.9,$ and varying $m \in (0, 1].$ Then, system (5) exhibits NK bifurcation at the critical value $m = m_h = 0.199023$ and has the equilibrium point $E^*(x^*, y^*) = (0.69031513, 2.24467052).$ Then, the characteristic (12) takes the following form:

$$\lambda^2 - 1.53322562\lambda + 1 = 0, \tag{72}$$

Then, the above characteristic polynomial has the eigenvalues $\lambda_{1,2} = 0.766613 \pm i0.64211.$ From (51), we obtain $\chi^* = -0.0946108.$ Then, the properties of NK bifurcation are illustrated in Theorem 2.

The interior equilibrium point varies for various values of $m,$ which is given in Table 2. The nature of system (5) near $E^*(x^*, y^*)$ is shown for different values of $m,$ for $m = 0.18$ is asymptotically stable, $m = 0.2, 0.5$ are invariant circles, $m = 0.58$ is period-8, $m = 0.88$ is invariant circle, and $m = 0.95$ is

locally asymptotically stable, as shown by the time plots in Figure 4 and the phase portraits in Figure 5. It shows that system (5) undergoes NK bifurcation and again attains stability via NK bifurcation. Also, the one parameter bifurcation diagram and the maximum Lyapunov exponent are shown in Figure 6.

6.1. Chaos Control. Next, we apply the state feedback control method for existing chaos in the flip bifurcation. The system (5) is in chaotic state for the parameter values in case (i), $r_1 = 3.3, a = 3.3, g = 1.2, b = 2.5, r_2 = 1, h = 0.525, c = 0.5$ and $m = 0.53.$ Then, $E^*(x^*, y^*) = (0.787379, 1.922151)$ is unstable, and its phase portrait is given in Figure 2(e). We need to shift the unstable equilibrium toward the stable state. For this, take $m = 0.53,$ and the corresponding controlled system is given by the following:

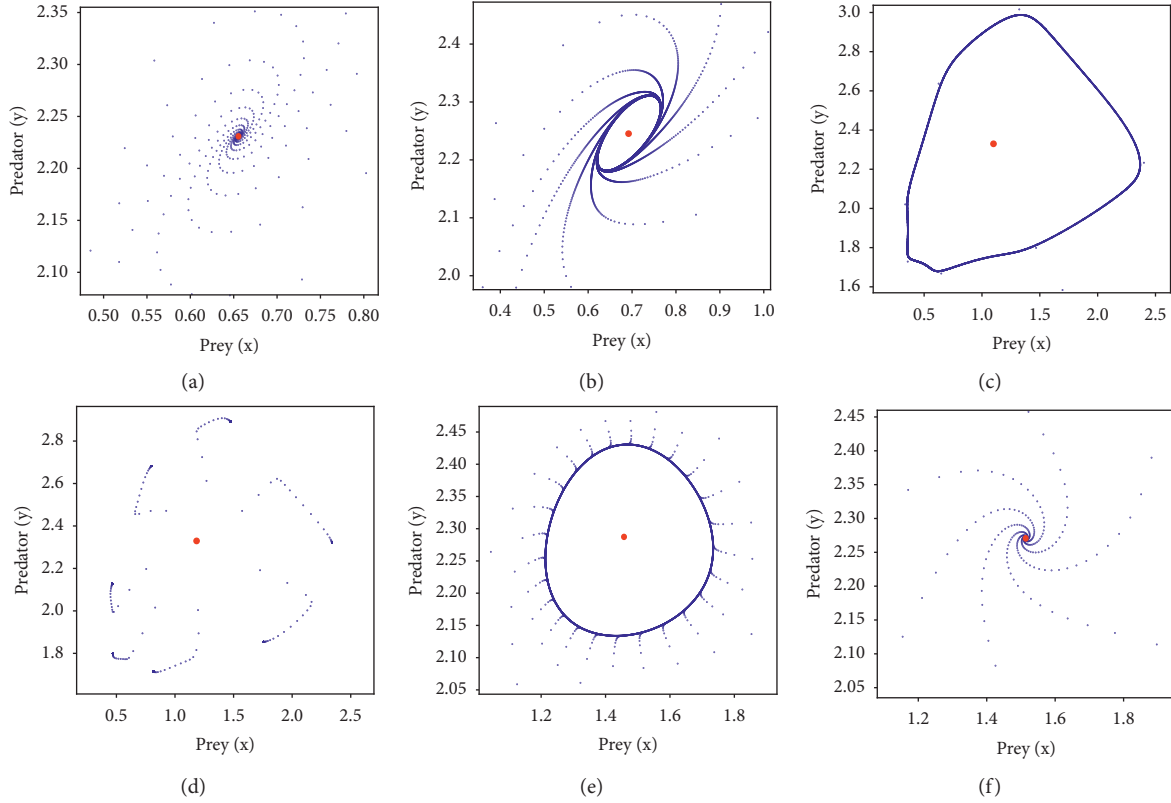


FIGURE 5: The phase portraits for system (5) with $r_1 = 4$, $a = 1.15$, $g = 2.7$, $b = 1.2$, $r_2 = 1$, $h = 1.06$, $c = 1.9$ (a) locally asymptotically stable for $m = 0.18$; ((b), (c)) invariant circles for $m = 0.2, 0.5$, (d) period-8 for $m = 0.58$, (e) invariant circle for $m = 0.88$, and (f) asymptotically stable for $m = 0.95$. The red points represent the interior equilibrium point $E^*(x^*, y^*)$, and its values are given in Table 2.

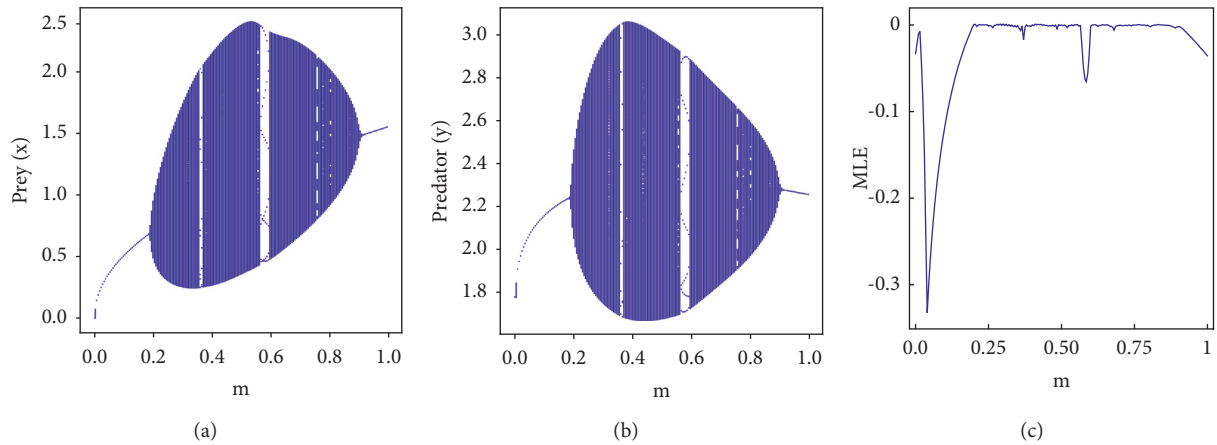


FIGURE 6: ((a), (b)). The Neimark-Sacker bifurcation diagram. (c) The maximum Lyapunov exponents for system (5) with $r_1 = 4$, $a = 1.15$, $g = 2.7$, $b = 1.2$, $r_2 = 1$, $h = 1.06$, $c = 1.9$, and $m \in [0, 1]$.

$$\begin{cases} x_{n+1} = x_n \exp \left[3.3 - 3.3x_n - \frac{1.2y_n}{x_n + 2.5} - u(x_n, y_n) \right], \\ y_{n+1} = y_n \exp \left[\frac{y_n}{y_n + 0.53} - \frac{0.525y_n}{x_n + 0.5} \right], \end{cases} \quad (73)$$

where $u(x_n, y_n) = h_1(x_n - x^*) + h_2(y_n - y^*)$, and h_1, h_2 are feedback gains. Furthermore, system (56) has the Jacobian matrix as follows:

$$J = \begin{pmatrix} -1.4303 - h_1 & -0.287419 - h_2 \\ 1.17037 & 0.385558 \end{pmatrix}. \quad (74)$$

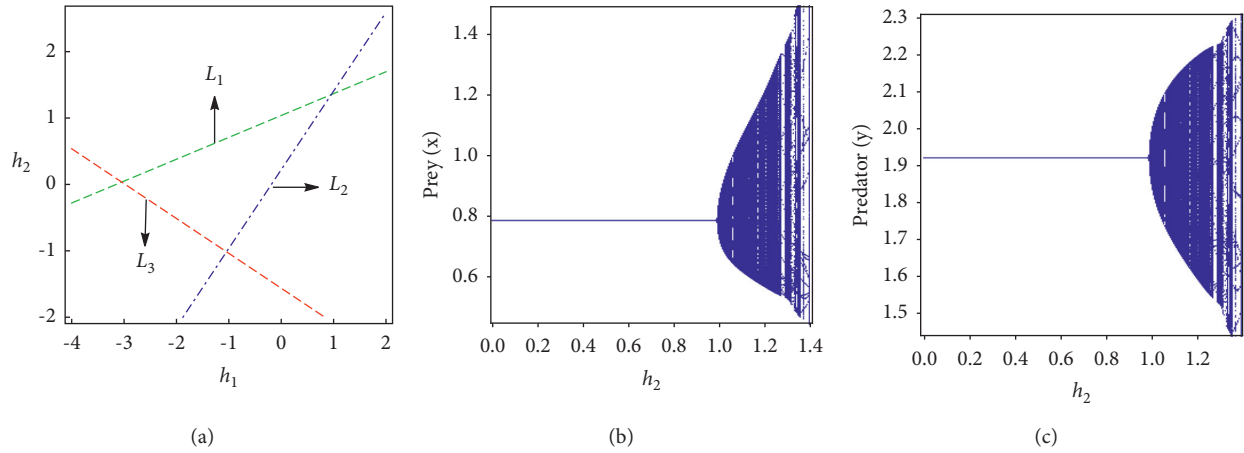


FIGURE 7: For the controlled system (36) with $r_1 = 3.3$, $a = 3.3$, $g = 1.2$, $b = 2.5$, $r_2 = 1$, $h = 0.525$, $c = 0.5$, $m = 0.53$, and $E^*(x^*, y^*) = (0.787379, 1.922151)$. (a) The stability triangle and ((b), (c) the bifurcation diagrams with $h_1 = -1$ and $h_2 = [0, 1.4]$.

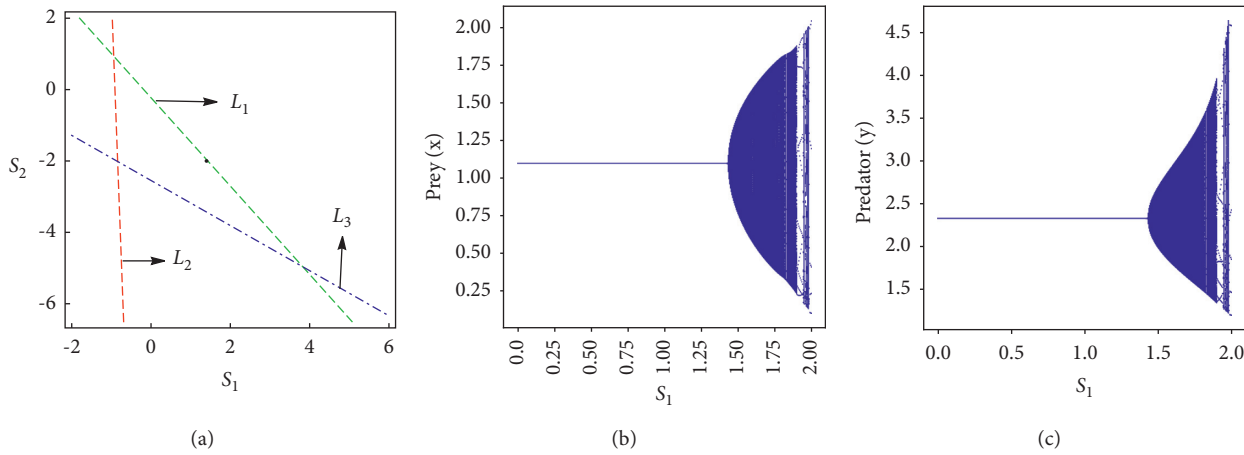


FIGURE 8: For the controlled system (48) with $r_1 = 4$, $a = 1.15$, $g = 2.7$, $b = 1.2$, $r_2 = 1$, $h = 1.06$, $c = 1.9$, $m = 0.5$, and $E^*(x^*, y^*) = (1.099589, 2.329801)$. (a) The stability triangle and ((b), (c) depict the bifurcation diagrams with $s_2 = -2$ and $s_1 = [0, 2]$.

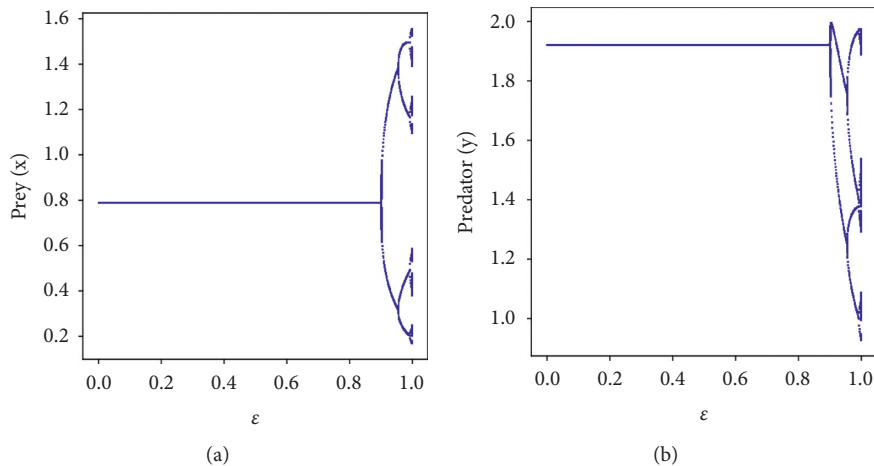


FIGURE 9: The bifurcation diagrams for the controlled system (54) with $r_1 = 3.3$, $a = 3.3$, $g = 1.2$, $b = 2.5$, $r_2 = 1$, $h = 0.525$, $c = 0.5$, $m = 0.53$, $E^*(x^*, y^*) = (0.787379, 1.922151)$, and $\epsilon \in (0, 1]$.

Then, we obtain the characteristic equation as follows:

$$\bar{\lambda}^2 + (1.04474 + h_1)\bar{\lambda} - 0.385558h_1 + 1.17037h_2 - 0.215078 = 0. \quad (75)$$

Furthermore, system (56) has the marginal stability lines, which are given by the following:

$$\begin{aligned} \bar{L}_1 &:= 0.38558h_1 - 1.17037h_2 = -1.21508, \\ \bar{L}_2 &:= 0.614442h_1 + 1.17037h_2 = -1.82966, \\ \bar{L}_3 &:= 1.38556h_1 - 1.17037h_2 = -0.259816. \end{aligned} \quad (76)$$

Then, the controlled system (56) has eigenvalues that may then be shown to be located within the triangular region defined by the straight lines \bar{L}_1 , \bar{L}_2 , and \bar{L}_3 (see Figure 7(a)). On choosing $k_1 = -1$, $E^*(x^*, y^*) = (0.787379, 1.922151)$ is locally stable if and only if $h_2 \in [-1, 0.8]$. Take $h_1 = -1$ and $h_2 \in [0, 1.4]$. Then, the bifurcation diagram for system (56) is plotted in Figures 7(b) and 7(c).

Secondly, we utilize the pole-placement control method by taking parameter values as in case (ii) $r_1 = 4$, $a = 1.15$, $g = 2.7$, $b = 1.2$, $r_2 = 1$, $h = 1.06$, $c = 1.9$, and $m = 0.5$. Then, system (5) is unstable near the equilibrium point $E^*(x^*, y^*) = (1.099589, 2.329801)$. To shift the unstable trajectory to the desired stable state, take $m = 0.5$, and system (48) is given by the following:

$$\begin{cases} x_{n+1} = x_n \exp\left[4 - 1.15x_n - \frac{2.7y_n}{x_n + 1.2}\right] = f_1(x_n, y_n), \\ y_{n+1} = y_n \exp\left[\frac{y_n}{0.5 - S + y_n} - \frac{1.06y_n}{x_n + 1.9}\right] = f_2(x_n, y_n), \end{cases} \quad (77)$$

where $S = s_1(x_n - x^*) + s_2(y_n - y^*)$, s_1 and s_2 are feedback gains. Then, we have the following:

$$\begin{aligned} A &= \begin{pmatrix} 1.04349 & -1.29105 \\ 0.63947 & 0.322162 \end{pmatrix}, \\ B &= \begin{pmatrix} 0 \\ -0.677838 \end{pmatrix}, \\ C &= \begin{pmatrix} 0 & 0.875124 \\ -0.677838 & -0.218374 \end{pmatrix}, \end{aligned} \quad (78)$$

and the above-controlled system has the Jacobian matrix, which is of the following form:

$$A - BK = \begin{pmatrix} 1.04349 & -1.29105 \\ 0.63947 + 0.677838s_1 & 0.322162 + 0.677838s_2 \end{pmatrix}, \quad (79)$$

and its characteristic polynomial is written as follows:

$$\bar{\lambda}^2 - (1.36565 + 0.677838s_2)\bar{\lambda} + 0.875124s_1 + 0.707315s_2 + 1.16176 = 0. \quad (80)$$

Furthermore, the lines of marginal stability of (77) are computed as follows:

$$\begin{aligned} L_1 &:= 1.16176 + 0.875124s_1 - 0.707315s_2 = 1, \\ L_2 &:= 2.16176 + 0.875124s_1 + 0.0294771s_2 = 1.36565, \\ L_3 &:= 3.52741 + 0.875124s_1 + 0.707315s_2 = -0.677838s_2. \end{aligned} \quad (81)$$

The eigenvalues may then be shown to be located within the triangular region defined by the straight lines \bar{L}_1 , \bar{L}_2 , and \bar{L}_3 for system (57) (see Figure 8(a)). On choosing $s_2 = -2$, $E^*(x^*, y^*)$ is locally asymptotically stable if and only if $s_1 \in [-0.84, 1.43]$. Take s_1 and $s_2 \in [0, 2]$. Then, the bifurcation diagrams for the controlled system (57) are depicted in figures 8(b) and 8(c).

Finally, we choose the parameter values as in case (i) $r_1 = 3.3$, $a = 3.3$, $g = 1.2$, $b = 2.5$, $r_2 = 1$, $h = 0.525$, $c = 0.5$, and $m = 0.53$ to explore the hybrid control strategy. Now, the controlled system (54) takes the following form:

$$\begin{cases} x_{n+1} = \epsilon x_n \exp\left[3.3 - 3.3x_n - \frac{1.2y_n}{x_n + 2.5}\right] + (1 - \epsilon)x_n, \\ y_{n+1} = \epsilon y_n \exp\left[\frac{y_n}{y_n + 0.53} - \frac{0.525y_n}{x_n + 0.5}\right] + (1 - \epsilon)y_n. \end{cases} \quad (82)$$

Moreover, we have $E^*(x^*, y^*) = (0.787379, 1.922151)$ for system (58), and its Jacobian matrix is written as follows:

$$\begin{pmatrix} 1 - 2.4303\epsilon & -0.28419\epsilon \\ 1.17037\epsilon & 1 - 0.614442\epsilon \end{pmatrix}. \quad (83)$$

If $(0 < \epsilon < 0.900535)$, then the above matrix has stable eigenvalues. Then, system (58) is stable near $E^*(x^*, y^*)$ for $(0 < \epsilon < 0.900535)$, which is depicted in the bifurcation diagram in Figure 9.

Remark 2. Allee effect could have a stabilizing or destabilizing effect or both, which depends on the parameters in the prey-predator model. For example, the growth of prey can cause chaotic dynamics in the discrete-time predator-prey model, and how the populations are changed from extinction to persistence because of the Allee effect in both prey and predator have been reported in [24]. The authors in [26] showed that without the Allee effect for a larger growth rate of prey, the system becomes chaotic near the boundary equilibrium point. In the presence of the Allee effect, the system becomes stable via reverse periodic doubling. Also, the considered system undergoes flip and Neimark–Sacker bifurcation near the interior equilibrium point at some critical Allee parameter value. System (5) considered in the present study has destabilizing effect for larger m , which is clearly shown in Figure 3. Also, with a different set of parameters, system (5) has both stabilizing and destabilizing effect because of m via Neimark–Sacker bifurcation, as shown in Figure 6.

Remark 3. Tassaddiq et al. [35] used a nonstandard finite difference scheme and obtained the discrete ratio-dependent prey-predator model. They showed that the considered system undergoes Neimark–Sacker bifurcation for larger values of the catchability coefficient. Moreover, they applied a pole-placement control strategy to obtain the controlled system and showed the controllable region in the feedback control space. Also, they applied the hybrid control strategy by choosing the catchability coefficient in the chaotic region and found the stability interval for the control parameter. Din [32] obtained the discrete system for (1) with a death rate of a predator by the method of piecewise constant arguments and showed that the considered system undergoes both types of bifurcations. Also, the author successfully implemented the state feedback control strategy to control FB and NSB and pole placement to control NSB. Hence, in the present study, we successfully implemented state feedback and hybrid control method to control FB, and the stable regions and bifurcation diagrams for feedback gains are shown in Figures 7 and 9 for system (5). Also, we implemented a pole-placement control method to control NSB, and it is depicted in Figure 8.

7. Conclusion

This article deals with a discrete-time modified Leslie–Gower system with the Allee effect in the predator population. The presence of the Allee effect in the prey-predator model can have a stabilizing or destabilizing effect. The existence criteria of biologically meaningful equilibrium points have been investigated, and their stability analysis has also been carried out. In system (1), even if the prey goes extinct, the predator can survive by changing its food habits and going for an alternative food source. Note that in system (5), the prey extinction equilibrium point $E_1 = (0, (r_2c/h) - m)$ exists only if $r_2c/h > m$, i.e., the Allee parameter m is certainly less than r_2c/h . Otherwise, the predator also goes to extinction in the absence of prey. In the absence of the Allee effect ($m = 0$), the prey extinction equilibrium point E_1 always exists. The existence and local stability of an interior equilibrium $E^* (x^*, y^*)$ can be achieved from Lemma 1 and Lemma 3. Figures 1(a), 4(a), and 4(f) show how the impact of m ensures the long-term survival of both species. We derived the conditions for the occurrence of flip and Neimark–Sacker bifurcations for system (5). Furthermore, we have discussed the direction and stability of both bifurcations with the help of the center manifold theorem and normal form theory. We showed that the size of the prey population increases and the predator population decreases when the Allee parameter m increases in Case (i), which is given in Table 1. Also, the sizes of both prey and predator populations increase when the Allee parameter m increases in Case (ii), which is given in Table 2. We showed that system (5) becomes chaotic from stable via flip bifurcation and also changes from stable to unstable via Neimark–Sacker bifurcation in numerical simulations for different sets of model parameters, varying the Allee parameter, see Figures 3 and 6. We verified the chaotic nature of the system with the help of a one-parameter bifurcation diagram and a

maximum Lyapunov exponent, which show the stabilizing and destabilizing effect of the Allee parameter m . We observed that the proposed system exhibits complex behavior and is sensitive to the choice of parameter values and initial conditions. The presence of complex and chaotic behaviors in system (5) by varying the Allee parameter m can cause both prey and predator populations to have a higher risk of extinction. The presence of chaotic behavior in system (5) affects the prediction of the sizes of both populations in future generations. Also, we showed that the state feedback, pole-placement, and hybrid control methods help to shift the unstable equilibrium to a stable state for a suitable range of control parameters in Figures 7, 8, and 9.

In short, the presence of the Allee effect on the predator population has a high impact on the dynamics of the modified Leslie–Gower system with populations that have no overlap between generations, resulting in a new discrete system (5) with various dynamical behaviors. Thus, it could be interesting and meaningful to study the dynamics of the discrete predator-prey system (5) with the Allee effects in both prey and predator, also with other interaction functions. However, these terms will increase the complexity of system (5), and we will leave this as future research.

Data Availability

Data sharing is not applicable to this article as no datasets were generated or analyzed during the current study.

Conflicts of Interest

The authors declare that they have no competing interests.

Authors' Contributions

All authors contributed equally and significantly in writing this paper and typed, read, and approved the final manuscript.

References

- [1] M. Danca, S. Codreanu, and B. Bakó, "Detailed analysis of a nonlinear prey-predator model," *Journal of Biological Physics*, vol. 23, no. 1, pp. 11–20, 1997.
- [2] R. M. May, "Biological populations with nonoverlapping generations: stable points, stable cycles, and chaos," *Science*, vol. 186, no. 4164, pp. 645–647, 1974.
- [3] H. I. Freedman, *Deterministic Mathematical Models in Population Ecology*, Wiley online library, Hoboken, New Jersey, USA, 1980.
- [4] Z. Jing and J. Yang, "Bifurcation and chaos in discrete-time predator-prey system," *Chaos, Solitons & Fractals*, vol. 27, no. 1, pp. 259–277, 2006.
- [5] X. Liu and D. Xiao, "Complex dynamic behaviors of a discrete-time predator-prey system," *Chaos, Solitons & Fractals*, vol. 32, no. 1, pp. 80–94, 2007.
- [6] A. Elalim, A. Elsadany, H. A. El-Metwally, E. M. Elabbasy, and H. N. Agiza, "Chaos and bifurcation of a nonlinear discrete prey-predator system," *Computational Ecology and Software*, vol. 2, no. 3, p. 169, 2012.

- [7] Z. He and X. Lai, "Bifurcation and chaotic behavior of a discrete-time predator-prey system," *Nonlinear Analysis: Real World Applications*, vol. 12, no. 1, pp. 403–417, 2011.
- [8] M. S. Shabbir, Q. Din, M. Safeer, M. A. Khan, and K. Ahmad, "A dynamically consistent nonstandard finite difference scheme for a predator-prey model," *Advances in Difference Equations*, vol. 381, no. 1, pp. 1–17, 2019.
- [9] R. E. Mickens, "A nonstandard finite-difference scheme for the Lotka-Volterra system," *Applied Numerical Mathematics*, vol. 45, no. 2-3, pp. 309–314, 2003.
- [10] L. Dai, *Nonlinear Dynamics of Piecewise Constant Systems and Implementation of Piecewise Constant Arguments*, World scientific, Singapore, 2008.
- [11] Q. Din, "Stability, bifurcation analysis and chaos control for a predator-prey system," *Journal of Vibration and Control*, vol. 25, no. 3, pp. 612–626, 2019.
- [12] M. A. Abbasi and Q. Din, "Under the influence of crowding effects: stability, bifurcation and chaos control for a discrete-time predator-prey model," *International Journal of Biomathematics*, vol. 12, no. 04, Article ID 1950044, 2019.
- [13] J. Dhar, H. Singh, and H. S. Bhatti, "Discrete-time dynamics of a system with crowding effect and predator partially dependent on prey," *Applied Mathematics and Computation*, vol. 252, pp. 324–335, 2015.
- [14] S. Pal, N. Pal, and J. Chattopadhyay, "Hunting cooperation in a discrete-time predator-prey system," *International Journal of Bifurcation and Chaos*, vol. 28, no. 07, Article ID 1850083, 2018.
- [15] H. N. Agiza, E. M. Elabbasy, H. El-Metwally, and A. A. Elsadany, "Chaotic dynamics of a discrete prey-predator model with Holling type II," *Nonlinear Analysis: Real World Applications*, vol. 10, no. 1, pp. 116–129, 2009.
- [16] W. E. Ricker, "Stock and recruitment," *Journal of the Fisheries Research Board of Canada*, vol. 11, no. 5, pp. 559–623, 1954.
- [17] J. D. Murray, *Mathematical Biology I. An Introduction*, Springer Science & Business Media, 2007, Berlin/Heidelberg, Germany, 2002.
- [18] W. C. Allee, *Animal Aggregations, a Study in General Sociology*, Univ. Press, Chicago, 1931.
- [19] M. Sen, M. Banerjee, and A. Morozov, "Bifurcation analysis of a ratio-dependent prey-predator model with the Allee effect," *Ecological Complexity*, vol. 11, pp. 12–27, 2012.
- [20] F. Peng and Y. Kang, "Dynamics of a modified Leslie-Gower model with double Allee effects," *Nonlinear Dynamics*, vol. 80, no. 1, pp. 1051–1062, 2015.
- [21] M. Sen and M. Banerjee, "Rich global dynamics in a prey-predator model with Allee effect and density dependent death rate of predator," *International Journal of Bifurcation and Chaos*, vol. 25, no. 03, Article ID 1530007, 2015.
- [22] S. Vinoth, R. Sivasamy, K. Sathiyathan et al., "Dynamical analysis of a delayed food chain model with additive Allee effect," *Advances in Difference Equations*, vol. 54, no. 1, pp. 1–20, 2021.
- [23] C. Çelik and O. Duman, "Allee effect in a discrete-time predator-prey system," *Chaos, Solitons & Fractals*, vol. 40, no. 4, pp. 1956–1962, 2009.
- [24] W. X. Wang, Y. B. Zhang, and C. Z. Liu, "Analysis of a discrete-time predator-prey system with Allee effect," *Ecological Complexity*, vol. 8, no. 1, pp. 81–85, 2011.
- [25] L. Cheng and H. Cao, "Bifurcation analysis of a discrete-time ratio-dependent predator-prey model with Allee effect," *Communications in Nonlinear Science and Numerical Simulation*, vol. 38, pp. 288–302, 2016.
- [26] Z. AlSharawi, S. Pal, N. Pal, and J. Chattopadhyay, "A discrete-time model with non-monotonic functional response and strong Allee effect in prey," *Journal of Difference Equations and Applications*, vol. 26, no. 3, pp. 404–431, 2020.
- [27] G. Chen and X. Dong, *From Chaos to Order: Methodologies, Perspectives and Applications*, World scientific, Singapore, 1998.
- [28] Y. A. Kuznetsov, *Elements of Applied Bifurcation Theory*, Springer, Berlin, Heidelberg, Germany, 2013.
- [29] L.-G. Yuan and Q.-G. Yang, "Bifurcation, invariant curve and hybrid control in a discrete-time predator-prey system," *Applied Mathematical Modelling*, vol. 39, no. 8, pp. 2345–2362, 2015.
- [30] S. Lynch, *Dynamical Systems with Applications Using python*, 2018.
- [31] E. Ott, C. Grebogi, and J. A. Yorke, "Controlling chaos," *Physical Review Letters*, vol. 64, no. 11, pp. 1196–1199, 1990.
- [32] Q. Din, "Complexity and chaos control in a discrete-time prey-predator model," *Communications in Nonlinear Science and Numerical Simulation*, vol. 49, pp. 113–134, 2017.
- [33] Q. Din, N. Saleem, and M. S. Shabbir, "A class of discrete predator-prey interaction with bifurcation analysis and chaos control," *Mathematical Modelling of Natural Phenomena*, vol. 15, p. 60, 2020.
- [34] M. Bilal Ajaz, U. Saeed, Q. Din, I. Ali, and M. I. Siddiqui, "Bifurcation analysis and chaos control in discrete-time modified Leslie-Gower prey harvesting model," *Advances in Difference Equations*, vol. 45, no. 1, pp. 1–24, 2020.
- [35] A. Tassaddiq, M. S. Shabbir, Q. Din, K. Ahmad, and S. Kazi, "A ratio-dependent nonlinear predator-prey model with certain dynamical results," *IEEE Access*, vol. 8, pp. 195074–195088, 2020.
- [36] M. A. Aziz-Alaoui and M. Daher Okiye, "Boundedness and global stability for a predator-prey model with modified Leslie-Gower and Holling-type II schemes," *Applied Mathematics Letters*, vol. 16, no. 7, pp. 1069–1075, 2003.
- [37] C. Ji, D. Jiang, and N. Shi, "Analysis of a predator-prey model with modified Leslie-Gower and Holling-type II schemes with stochastic perturbation," *Journal of Mathematical Analysis and Applications*, vol. 359, no. 2, pp. 482–498, 2009.
- [38] C. Ji, D. Jiang, and N. Shi, "A note on a predator-prey model with modified Leslie-Gower and Holling-type II schemes with stochastic perturbation," *Journal of Mathematical Analysis and Applications*, vol. 377, no. 1, pp. 435–440, 2011.
- [39] H. Singh, J. Dhar, and H. Singh Bhatti, "Discrete-time bifurcation behavior of a prey-predator system with generalized predator," *Advances in Difference Equations*, vol. 206, no. 1, pp. 1–15, 2015.
- [40] W. Liu and D. Cai, "Bifurcation, chaos analysis and control in a discrete-time predator-prey system," *Advances in Difference Equations*, vol. 11, no. 1, pp. 1–22, 2019.
- [41] S. Vinoth, R. Sivasamy, K. Sathiyathan et al., "The dynamics of a leslie type predator-prey model with fear and Allee effect," *Advances in Difference Equations*, vol. 338, no. 1, pp. 1–22, 2021.
- [42] J. Guckenheimer and P. Holmes, *Nonlinear Oscillations, Dynamical Systems, and Bifurcations of Vector fields*, Springer, Berlin, Heidelberg, Germany, 2013.
- [43] C. Robinson, *Dynamical Systems: Stability, Symbolic Dynamics, and Chaos*, Routledge, Oxfordshire, England, UK, 1998.